CONTRACT REPORT ARBRL-CR-00373

EPIC-2, A COMPUTER PROGRAM FOR
ELASTIC - PLASTIC IMPACT COMPUTATIONS
IN 2 DIMENSIONS PLUS SPIN

Prepared by

Honeywell, Inc.
Defense Systems Division
600 Second Street Northeast
Hopkins, Minnesota 55343

June 1978

US ARMY ARMAMENT RESEARCH AND DEVELOPMENT COMMAND
BALLISTIC RESEARCH LABORATORY
ABERDEEN PROVING GROUND, MARYLAND

78 08 09 099

Destroy this report when it is no longer needed.
Do not return it to the originator.

(18) ARBRL, SBIE/   (19) CR-00373, AD E430 097

SECURITY CLASSIFICATION OF THIS PAGE (When Data Entered)

REPORT DOCUMENTATION PAGE	READ INSTRUCTIONS BEFORE COMPLETING FORM	
1 REPORT NUMBER CONTRACT REPORT ARBRL-CR-00373	2 GOVT ACCESSION NO	3 RECIPIENT'S CATALOG NUMBER
4 TITLE (and Subtitle) EPIC-2, A Computer Program for Elastic-Plastic Impact Computations in 2 Dimensions Plus Spin		5 TYPE OF REPORT & PERIOD COVERED Final Feb 1977 - Dec 1977
		6 PERFORMING ORG. REPORT NUMBER 41154
7 AUTHOR(s) Gordon R. Johnson		8 CONTRACT OR GRANT NUMBER(s) DAAD05-77-C-0730
9 PERFORMING ORGANIZATION NAME AND ADDRESS Honeywell Inc., Defense Systems Division 600 Second Street Northeast Hopkins, Minnesota 55343		10 PROGRAM ELEMENT PROJECT, TASK AREA & WORK UNIT NUMBERS
11 CONTROLLING OFFICE NAME AND ADDRESS US Army Armament Research & Development Command US Army Ballistic Research Laboratory (DRDAR-BL) Aberdeen Proving Ground, MD 21005		12 REPORT DATE JUNE 1978
		13 NUMBER OF PAGES 84
14 MONITORING AGENCY NAME & ADDRESS(if different from Controlling Office)		15 SECURITY CLASS (of this report) UNCLASSIFIED
		15a DECLASSIFICATION DOWNGRADING SCHEDULE

16 DISTRIBUTION STATEMENT (of this Report)

Approved for public release; distribution unlimited.

17 DISTRIBUTION STATEMENT (of the abstract entered in Block 20, if different from Report)

18 SUPPLEMENTARY NOTES

19 KEY WORDS (Continue on reverse side if necessary and identify by block number)

Impact	Lagrangian
Penetration	Elastic-Plastic
Wave Projagation	Hydrodynamic
Finite Element	Explosive Detonation

20 ABSTRACT (Continue on reverse side if necessary and identify by block number)

A two-dimensional (plus spin) computer program, EPIC-2, is described for impact and explosive detonation problems. The numerical technique is based on a Lagrangian finite element formulation in which the equations of motion are integrated directly rather than through the traditional stiffness matrix approach. Triangular elements are formulated for large strains and displacements, and nonlinear material strength and compressibility effects are included to account for elastic-plastic flow and wave propagation. Instructions for using the program are also included.

DD FORM 1473 EDITION OF 1 NOV 65 IS OBSOLETE
1 JAN 73

SECURITY CLASSIFICATION OF THIS PAGE (When Data Entered)

393 249   78 08 09 099

FOREWORD

CONTENTS

ILLUSTRATIONS

SECTION 1
INTRODUCTION AND SUMMARY

This report documents a computer code for dynamic analyses of impact and explosive detonation problems. The code, EPIC-2 (Elastic-Plastic Impact Computations in 2 dimensions) is applicable for axi-symmetric and plane strain problems. It also has the ability to handle the effect of spin for the axi-symmetric case. It is based on a Lagrangian finite element formulation where the equations of motion are integrated directly, rather than through the traditional stiffness matrix approach. Nonlinear material strength and compressibility effects are included to account for elastic-plastic flow and wave propagation. An option to include high explosives is also available. Although the code is arranged to provide solutions for projectile-target impact, and explosive detonation problems, the basic formulation is valid for a wide range of problems involving dynamic responses of continuous media.

The EPIC-2 code has material descriptions which include strain hardening, strain rate effects, thermal softening and fracture. Geometry generators are included to quickly generate flat plates, spheres and rods with blunt, rounded or conical nose shapes. It has the capacity to include multiple sliding surfaces, it is restartable, and it provides plots of initial and deformed geometry as well as strain, stress, pressure and velocity fields. Time-dependent plots of various system parameters are also available.

A desirable characteristic of this technique is that there is no need to provide an orderly arrangement of nodes as is required for finite-difference techniques. Complex geometrical shapes can be represented simply by providing an adequate assemblage of elements to represent the geometry. Various boundary conditions can also be represented in a straightforward manner. Another desirable characteristic is that this technique is formulated

for a triangular element, which is well suited to represent the severe distortions which often occur during high-velocity impact. A triangular element also provides a state of constant strain such that all material in an element behaves uniformly. This allows for an accurate and convenient selection of a constant stress within the element.

This report includes a complete description and formulation of the EPIC-2 computer code. Detailed instructions for using this code are also provided.

SECTION 2
FORMULATION

The EPIC-2 computational technique for axi-symmetric impact problems is shown in Figure 1. The first step in the process is to represent the geometry with triangular elements having specific material characteristics. Then the distributed mass is lumped at the nodes (element corners), and initial velocities are assigned to represent the motion at impact. If the problem involves explosive detonation, there may be no initial velocities and the initial conditions are established by allowing the detonation process to begin at a predetermined point.
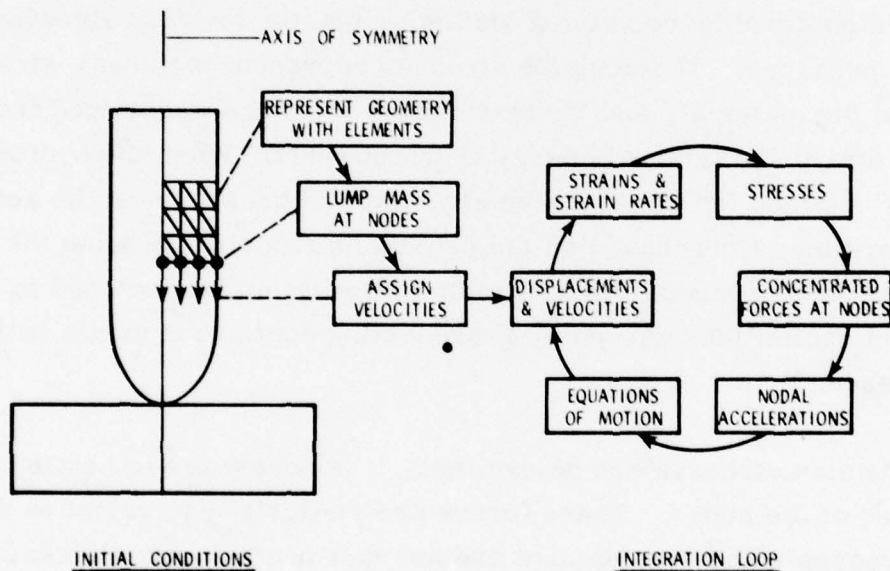
Figure 1. Schematic Representation of the Finite Element Computational Technique

3

After the initial conditions are established, the integration loop begins as shown in Figure 1. The first step is to obtain displacements and velocities of the nodes. If it is assumed the lines connecting the nodes (element edges) remain straight, then the displacements and velocities within the elements must vary linearly. From these displacements and velocities, the strains and strain rates within the elements can be obtained. Since the strains and strain rates are generally derivatives of linear displacement and velocity functions within the elements, the resulting strains and strain rates are generally constant within the elements.

The stresses in the elements are determined from the strains, strain rates, internal energies and material properties. Since the strains and strain rates are constant within the elements, the stresses are also constant. The stresses are obtained by combining elastic or plastic deviator stresses with hydrostatic pressure. The deviator stresses represent the shear-strength capability of the material, and the hydrostatic pressure is obtained from the volumetric strain and internal energy of the element. When the hydrostatic pressure is obtained for an explosive element, the pressure can be activated at a predetermined time (based on the detonation velocity) or when the element is sufficiently compressed. An artificial viscosity is also included to damp out localized oscillations caused by representing continuous media with lumped masses.

After the element stresses are determined, it is necessary to obtain concentrated forces at the nodes. These forces are statically equivalent to the distributed stresses within the element and are dependent on the element geometry and the magnitude of the stresses. When the concentrated forces are applied to the concentrated masses, the nodal accelerations are defined, and the equations of motion are applied to determine new displacements and velocities. The integration loop is then repeated until the time of interest has elapsed.

Another feature of the basic technique is the ability to represent sliding be-
tween two surfaces. This is accomplished with a momentum exchange
principle which allows for closing, sliding and separation of two surfaces.
It should be noted that the integration time increment must be properly con-
trolled to prevent numerical instability. This is accomplished by limiting
the time increment to a fraction of the time required to travel across the
minimum altitude of the element at the sound velocity of the material. This
also ensures that the time increment is less than the shortest period of
vibration of the system.

2.1 GEOMETRY

A typical axi-symmetric triangular element is shown in Figure 2. It is geo-
metrically defined by nodes i, j and m, with the mass of the element being
equally distributed to concentrated masses at the nodes. When a node is
contained by more than one element, the total mass at node i, $\overline{M}_i$, is equal
to 1/3 the mass of all elements which contain that node. For an axi-symmetric
finite element model, the concentrated masses can be visualized as concen-
tric circular rings contained in planes which are perpendicular to the axis of
revolution. These rings can move up and down along the axial direction
(Z axis) and they can expand and contract in the radial direction (R axis).
In addition, they are allowed to experience rotations θ about the axis of
revolution. The coordinates of node i are designated r_i, z_i, θ_i, and the
radial, axial and tangential velocities are designated $\dot{u}_i$, $\dot{v}_i$, $\dot{w}_i$, where
$\dot{w}_i = r_i \dot{\theta}_i$.

5
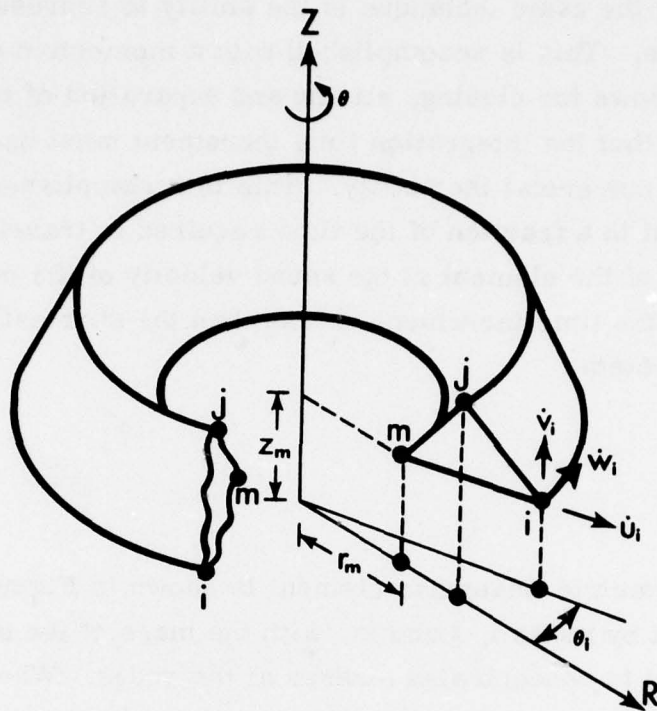
Figure 2. Geometry of an Axisymmetric Element

2.2 STRAINS AND STRAIN RATES

The incremental strains which occur during each cycle of integration are obtained by multiplying the strain rates by the integration time increment. The strain rates are obtained from the current geometry of the element and the velocities of the nodes. If it is assumed that the lines connecting the nodes remain straight, the displacements and velocities within each element must vary in a linear manner. Then the velocities within the element can be expressed as

$$\dot{u} = \alpha_1 + \alpha_2 r + \alpha_3 z \tag{1}$$

$$\dot{v} = \alpha_4 + \alpha_5 r + \alpha_6 z \tag{2}$$

$$\dot{w} = \alpha_7 + \alpha_8 r + \alpha_9 z \tag{3}$$

where $\alpha_1 \ldots \alpha_9$ are geometry and velocity-dependent constants. It is possible to solve for α_1, α_2, α_3 by substituting the radial velocities and coordinates of nodes i, j, m into Equation (1). This gives three equations and three unknowns such that Equation (1) can be expressed in terms of the element geometry and nodal velocities.

$$\dot{u} = \frac{1}{2A}[(a_i + b_i r + c_i z)\dot{u}_i + (a_j + b_j r + c_j z)\dot{u}_j + (a_m + b_m r + c_m z)\dot{u}_m] \tag{4}$$

where $a_i = r_j z_m - r_m z_j$, $b_i = z_j - z_m$, $c_i = r_m - r_j$, and A is the cross-sectional area of the element in the R-Z plane. The other velocities ($\dot{v}$, $\dot{w}$) are identical to Equation (4) except the radial velocities are replaced by the axial and tangential velocities.

After the velocities are obtained, it is possible to determine the normal strain rates ($\dot{\epsilon}_r$, $\dot{\epsilon}_z$, $\dot{\epsilon}_\theta$), the shear strain rates ($\dot{\gamma}_{rz}$, $\dot{\gamma}_{r\theta}$, $\dot{\gamma}_{z\theta}$) and the localized rotational spin rate of the element in the R-Z plane (ω_{rz}).

$$\dot{\epsilon}_r = \frac{\partial \dot{u}}{\partial r} \tag{5}$$

$$\dot{\epsilon}_z = \frac{\partial \dot{v}}{\partial z} \tag{6}$$

$$\dot{\epsilon}_\theta = \frac{\bar{\dot{u}}}{r} \tag{7}$$

$$\dot{\gamma}_{rz} = \frac{\partial \dot{u}}{\partial z} + \frac{\partial \dot{v}}{\partial r} \tag{8}$$

$$\dot{\gamma}_{r\theta} = \frac{\partial \dot{w}}{\partial r} - \frac{\bar{\dot{w}}}{r} \tag{9}$$

7

$$\dot{\gamma}_{z\theta} = \frac{\partial \dot{w}}{\partial z} \tag{10}$$

$$\omega_{rz} = \frac{1}{2}\left(\frac{\partial \dot{v}}{\partial r} - \frac{\partial \dot{u}}{\partial z}\right) \tag{11}$$

It can be seen that Equations (5), (6), (8), (10) and (11) are derivatives of linear functions and are therefore constant within the element. Equations (7) and (9) involve averages of the nodal velocities ($\bar{u}$ and $\bar{w}$) and the three radii ($\bar{r}$), so they are not necessarily constant. It is also necessary to use an equivalent strain rate which is expressed as

$$\bar{\dot{\epsilon}} = \sqrt{\frac{2}{9}\left[(\dot{\epsilon}_r - \dot{\epsilon}_z)^2 + (\dot{\epsilon}_r - \dot{\epsilon}_\theta)^2 + (\dot{\epsilon}_z - \dot{\epsilon}_\theta)^2 + \frac{3}{2}(\dot{\gamma}_{rz}^2 + \dot{\gamma}_{r\theta}^2 + \dot{\gamma}_{z\theta}^2)\right]} \tag{12}$$

An equivalent plastic strain, $\bar{\epsilon}_p$, is then obtained by integrating $\bar{\dot{\epsilon}}$ with respect to time during plastic flow.

$$\bar{\epsilon}_p^{t+\Delta t} = \bar{\epsilon}_p^t + \bar{\dot{\epsilon}}\Delta t \tag{13}$$

where Δt is the integration time increment. It should also be noted that subsequent computations will involve deviator strain rates ($\dot{e}_r$, $\dot{e}_z$, $\dot{e}_\theta$) which are readily obtained from the normal strain rates ($\dot{\epsilon}_r$, $\dot{\epsilon}_z$, $\dot{\epsilon}_\theta$).

2.3 STRESSES AND PRESSURES

The stresses in the elements are determined from the strains, strain rates, internal energies and material properties. The three normal stresses (σ_r, σ_z, σ_θ) are expressed in terms of deviator stresses (s_r, s_z, s_θ) hydrostatic pressure, P, and artifical viscosity Q.

$$\sigma_r = s_r - (P + Q) \tag{14}$$

$$\sigma_z = s_z - (P + Q) \tag{15}$$

$$\sigma_\theta = s_\theta - (P + Q) \tag{16}$$

Trial values of the deviator stresses at time $= t + \Delta t$ are

$$s_r^{t+\Delta t} = s_r^t + 2G\dot{e}_r \Delta t - 2\tau_{rz}^t \omega_{rz} \Delta t \tag{17}$$

$$s_z^{t+\Delta t} = s_z^t + 2G\dot{e}_z \Delta t + 2\tau_{rz}^t \omega_{rz} \Delta t \tag{18}$$

$$s_\theta^{t+\Delta t} = s_\theta^t + 2G\dot{e}_\theta \Delta t \tag{19}$$

In Equation (17) the first term (s_r^t) is the radial stress at the previous time and the second term $(2G\dot{e}_r \Delta t)$ is the incremental stress due to the incremental strain $(\dot{e}_r \Delta t)$ during that time increment, where G is the elastic shear modulus. The third term $(2\tau_{rz}^t \omega_{rz} \Delta t)$ is due to shear stresses from the previous time increment, which now act as normal stresses due to the new orientation of the element caused by an incremental rotation $(\omega_{rz} \Delta t)$ during the time increment. The axial stress has the same form as the radial stress, and tangential stress is also similar except there is no contribution from rotated shear stresses.

The trial values of the shear stresses are formulated in similar manner.

$$\tau_{rz}^{t+\Delta t} = \tau_{rz}^t + G\dot{\gamma}_{rz} \Delta t + (\sigma_r^t - \sigma_z^t) \omega_{rz} \Delta t \tag{20}$$

$$\tau_{r\theta}^{t+\Delta t} = \tau_{r\theta}^t + G\dot{\gamma}_{r\theta} \Delta t \tag{21}$$

$$\tau_{z\theta}^{t+\Delta t} = \tau_{z\theta}^t + G\dot{\gamma}_{z\theta} \Delta t \tag{22}$$

9

The rotational terms can only be significant for stresses in the R-Z plane since the elements can rotate without experiencing strain rates. For the other stresses involving θ, the analogous rotations cannot occur without inducing strain rates, and the effect of the rotational-induced stresses is small compared to the strain rate induced stresses.

It should be recalled that Equations (17) through (22) represent trial values of the stresses and they may need to be reduced if they violate the Von Mises yield criterion. An equivalent stress is given by

$$\bar{\sigma} = \sqrt{\frac{3}{2}(s_r^2 + s_z^2 + s_\theta^2) + 3(\tau_{rz}^2 + \tau_{r\theta}^2 + \tau_{z\theta}^2)} \tag{23}$$

If $\bar{\sigma}$ is not greater than the equivalent tensile strength of the material, $\bar{S}$, the final deviator and shear stresses are as given in Equations (17) through (22). If $\bar{\sigma}$ is greater than $\bar{S}$, then the stresses in Equations (17) through (22) should be multiplied by the factor $(\bar{S}/\bar{\sigma})$. When the reduced deviator and shear stresses are put into Equation (23), the result is always $\bar{\sigma} = \bar{S}$.

The equivalent tensile strength of the material may be dependent on many factors, including strain, strain rate, pressure and temperature. It is well-known that many materials behave differently under dynamic impact than under static testing conditions. With few exceptions, however, a precise definition of material behavior under dynamic conditions is not available. There is also much to be learned about fracture characteristics under these dynamic conditions. The current version of EPIC-2 allows the equivalent tensile strength to be determined from

$$\bar{S} = S_{\bar{\varepsilon}_p} [1 + C_1 \log(\bar{\dot{\varepsilon}})] [1 + C_2 \bar{P} + C_3 \bar{P}^2] [C_4 + C_5 T] \tag{24}$$

In this formulation, $S_{\bar{\varepsilon}_p}$ is generally taken to be the static stress, which is dependent on the equivalent plastic strain of Equation (13). The three bracketed terms allow the static stress to be altered, based on strain rate,

10

pressure and temperature. If the constants are $C_1 = C_2 = C_3 = C_5 = 0$ and $C_4 = 1.0$, then $\bar{S} = S_{\bar{\epsilon}_p}$, which is the strain-dependent static stress. The first bracketed term can increase the strength due to the equivalent strain rate, $\dot{\bar{\epsilon}}$, described in Equation (12). In the second bracketed term, $\bar{P} = P + Q$, so the effect of this term is to increase the strength due to pressure. The final bracketed term includes the temperature, T, of the element, which is obtained from

$$T = T_o + \frac{E_s}{C_s \rho_o} \tag{25}$$

where T_o is the initial temperature of the element, E_s is the internal energy per original unit volume (defined later), C_s is the specific heat and ρ_o is the initial density.

Material fracture is currently dependent on the equivalent plastic strain $\bar{\epsilon}_p$. (Equation 13) and the volumetric strain, $\epsilon_v = V/V_o - 1$, where V and V_o represent the current and initial volumes of the element. When the fracture criterion has been met, the equivalent tensile stress is set equal to zero, so no shear stresses can be developed in the failed element. Likewise, no tensile stresses are allowed to develop. The net result is that a failed element tends to act like a liquid inasmuch as it can develop only hydrostatic compression with no shear or tensile stresses. Another option is also available which sets all stresses (including the pressure) equal to zero.

The hydrostatic pressure is dependent on the volumetric strain and the internal energy in the element. The EPIC-2 code uses the Mie-Grüneisen equation of state in the general form $P = P_v + \Gamma E_s (1+\mu)$, with the complete expression given by

$$P = (K_1\mu + K_2\mu^2 + K_3\mu^3)(1 - \frac{\Gamma\mu}{2}) + \Gamma E_s (1 + \mu) \tag{26}$$

11

where $\mu = V_o/V - 1$, K_1, K_2, and K_3 are material-dependent constants and Γ is the Grüneisen coefficient.

Since the pressure can be significantly affected by the internal energy E_s, it is desirable to solve the pressure and energy equations simultaneously. This gives

$$E_s^{t+\Delta t} = \frac{E_s^t - .5\left[(P+Q)^t + Q^{t+\Delta t} + P_v^{t+\Delta t}\right]\dot{\epsilon}_v\Delta t + \Delta E_d}{1 + .5\,\Gamma(1+\mu)\,\dot{\epsilon}_v\Delta t} \qquad (27)$$

where $\dot{\epsilon}_v$ is the volumetric strain rate and ΔE_d is the internal energy generated by the deviator and shear stresses during the previous cycle.

$$\Delta E_d = (\bar{s}_r\dot{e}_r + \bar{s}_z\dot{e}_z + \bar{s}_\theta\dot{e}_\theta + \bar{\tau}_{rz}\dot{\gamma}_{rz} + \bar{\tau}_{r\theta}\dot{\gamma}_{r\theta} + \bar{\tau}_{z\theta}\dot{\gamma}_{z\theta})$$

$$(\bar{V}/V_o)\,\Delta t \qquad (28)$$

The "bars" on the deviator and shear stresses, and the volume, represent averages of these values at times t and $t+\Delta t$. After the total internal energy at time $t+\Delta t$ has been determined from Equation (27), the pressure at time $t+\Delta t$ is determined from Equation (26).

For explosive detonation, the hydrostatic pressure is determined by a procedure similar to that used in the HEMP code.[1] The pressure, determined by the Gamma Law, is given by

$$P = F(\gamma - 1)E_s(1 + \mu) \qquad (29)$$

where F is the burn fraction ($0 \leq F \leq 1.0$), γ is a material constant, and E_s is the internal energy per initial unit volume. Unlike the solid and liquid materials, the explosive contains internal energy in the initial condition. The pressure and energy equations are solved simultaneously in a manner

12

similar to that of Equations (26) and (27). The explosive is effectively initiated with the burn fraction, which is dependent on the time for detonation to arrive and travel through the element, or the compressed state of the element. The burn fractions for these two conditions are

$$F = \frac{(t_s - t) D}{4\sqrt{A_o}} \tag{30a}$$

$$F = \frac{1 - V/V_o}{1 - V_{CJ}} \tag{30b}$$

In Equation 30a, A_o is the initial area of the element and t_s is the time required for the detonation wave to reach the node closest to the point of initiation when traveling at the detonation velocity, D. This formulation tends to spread the wave front over a limited number of elements. Equation 30b gives the burn fraction in terms of the compressed state, where $V_{CJ} = \frac{\gamma}{\gamma + 1}$ is the Chapman-Jouquet relative volume. This allows a converging detonation wave to travel at a velocity greater than D. The minimum and maximum allowable values of F are 0. and 1.0.

The artificial viscosity is combined with the normal stresses to damp out localized oscillations of the concentrated masses. It tends to eliminate spurious oscillations which would otherwise occur for wave propagation problems. This technique was originally proposed by Von Neumann and Richtmyer[2] and has been expanded for use in various computer codes.[3] It is expressed in terms of linear and quadratic components and is applied only when the volumetric strain rate is negative:

$$Q = C_L \rho c_s h \, |\dot{\epsilon}_v| + C_o^2 \rho h^2 (\dot{\epsilon}_v)^2 \quad \text{for } \dot{\epsilon}_v < 0$$

$$Q = 0 \quad \text{for } \dot{\epsilon}_v \geq 0 \tag{31}$$

13

where c_s and ρ are the sound velocity and density of the material and h is the minimum altitude of the triangle. Typical values used for the dimensionless coefficients are $C_L = 0.5$ and $C_o^2 = 4.0$.[1]

The sound velocity for solid and liquid elements[4] is obtained from

$$c_s^2 = \frac{1}{\rho_o} [K_1 (1 - \Gamma\mu) + K_2 (2\mu - 1.5\Gamma\mu^2) + K_3 (3\mu^2 - 2\Gamma\mu^3)$$
$$+ \Gamma E_s + \Gamma\bar{P}/(1+\mu)] \tag{32}$$

and the sound velocity for explosive elements is obtained from

$$c_s^2 = \frac{\gamma\bar{P}}{\rho} \tag{33}$$

The sound velocities are also used for determination of the integration time increment.

2.4 CONCENTRATED FORCES

After the element stresses are obtained, it is necessary to determine concentrated forces to act on the concentrated mass at the nodes. This is done by obtaining the concentrated forces which are statically equivalent to the distributed stresses in the elements. The radial, axial and tangential forces acting on node i of an element, are

$$F_r^i = -\pi\bar{r} \left[(z_j - z_m)\sigma_r + (r_m - r_j)\tau_{rz} \right] - \frac{2}{3}\pi A \sigma_\theta \tag{34}$$

$$F_z^i = -\pi\bar{r} \left[(r_m - r_j)\sigma_z + (z_j - z_m)\tau_{rz} \right] \tag{35}$$

14

$$F_\theta^i = -\pi\bar{r}\left[\frac{\bar{r}}{r_i}(z_j - z_m)\tau_{r\theta} + (r_m - r_j)\tau_{z\theta}\right] \tag{36}$$

In Equation (36) the factor $\bar{r}/r_i$ is included in the expression involving the shear stress in the R-θ plane. This is necessary to satisfy the equilibrium condition in this plane which is $\frac{\partial\tau_{r\theta}}{\partial r} + \frac{2\tau_{r\theta}}{r} = 0$.[5] It is clear from this condition that the shear stress cannot be a non-zero constant, but rather must vary as a function of the radius. This stress is obtained from $\dot{\gamma}_{r\theta}$ in Equation (9) and is not necessarily constant since it involves averages of the three nodal displacements and radii. Therefore, the factor $\bar{r}/r_i$ in Equation (36) represents the effect of a variable-shear stress in the element. The net forces at node i ($\bar{F}_r^i$, $\bar{F}_z^i$, $\bar{F}_\theta^i$) are the sum of the forces from each of the individual element forces at that node.

2.5 EQUATIONS OF MOTION

The equations of motion are integrated by assuming a constant velocity for each time increment. The acceleration of node i in the radial direction at time = t is

$$\ddot{u}_i^t = \frac{\bar{F}_r^i}{M_i} + r_i^t\left(\dot{\theta}_i^{t-}\right)^2 \tag{37}$$

The first term is due to stress-induced forces and the second term is due to spin. The updated velocity for the next time increment is

$$\dot{u}_i^{t+} = (\dot{u}_i^{t-} + \ddot{u}_i^t\,\overline{\Delta t})\,(1 - C_D\,\overline{\Delta t}/r_i^t) \tag{38}$$

where $\dot{u}_i^{t-}$ is the constant velocity for the previous time increment and $\overline{\Delta t}$ is the average of the two integration time increments about time = t. The expression in the second set of parentheses can be used to damp out the radial

15

velocities to give steady-state solutions for spinning bodies. If the constant, C_D, is set equal to twice the sound velocity of the material, the system will be approximately critically damped and the steady-state solution will be rapidly attained. This will later be demonstrated in an example. Finally, the new radial displacement at time = t+Δt is

$$u_i^{t+\Delta t} = u_i^t + \dot{u}_i^{t+} \, \Delta t \tag{39}$$

The equations of motion for the axial direction have a similar form except the spin effects for the acceleration and the damping effects for the velocity are not included.

For the circumferential equations of motion it is necessary to consider the angular momentum, H, of each concentrated mass. This gives

$$H_i^{t+} = H_i^{t-} + r_i^t \, \overline{F}_\theta^i \, \overline{\Delta t} \tag{40}$$

By substituting $H_i = \dot{\theta}_i \, r_i^2 \, \overline{M}_i$ into Equation (40), it is possible to determine the updated rotation velocity.

$$\dot{\theta}_i^{t+} = \dot{\theta}_i^{t-} \left(\frac{r_i^t}{r_i^{t+\Delta t}} \right)^2 + \frac{r_i^t \, \overline{\Delta t}}{(r_i^{t+\Delta t})^2} \left(\frac{\overline{F}_\theta^i}{\overline{M}_i} \right) \tag{41}$$

It should be noted that even if the net circumferential force, $\overline{F}_\theta^i$ is equal to zero, it is possible for the spin to change if the radius changes between times t and t+Δt. It is therefore necessary to obtain the new radial position at t+Δt before obtaining the new rotation velocity at t+Δt.

The integration time increment must be controlled to prevent numerical instability. This is done by limiting the time increment to

16

$$\Delta t = C_t \left[\frac{h_{min}}{\sqrt{g^2} + \sqrt{g^2 + c_s^2}} \right] \qquad (42)$$

where $g^2 = C_o^2 Q/\rho$, h_{min} is the minimum altitude of the triangle and c_s is the sound velocity.[3] The constant, C_t, must be less than unity to ensure that Δt is always less than the time required to travel across the shortest dimension of the triangle at the sound velocity of the material. This criterion also ensures that Δt is less than the lowest period of vibration of the system.[6] The EPIC-2 program restricts the time increment from increasing more than 10 percent per cycle.

2.6 SLIDING SURFACES

It is sometimes necessary to allow for sliding to occur between two surfaces. The important steps for the sliding-surface technique are summarized as follows:

- Identify a "master" sliding surface defined by a specified row of master nodes.

- Identify a "slave" surface (or region) defined by a specific row (or group) of slave nodes. The slave node spacing should not be significantly greater than the master node spacing since this could introduce localized deformations in the master surface at the slave node locations.

- For each integration time increment, apply the equations of motion to both the master nodes and the slave nodes in the usual manner.

- For each slave node, find the portion of the master surface (defined by two master nodes) whose projection contains that slave node.

17

- Check to determine if there is interference between the slave node and the master surface.

- If there is interference, place the slave node on the master surface in a direction normal to the master surface.

- Determine the translational momentum of the two master nodes and the slave node in a direction normal to the master surface. Also determine the angular momentum of these three nodes about a point on a line which contains the two master nodes.

- Determine updated velocities of the two master nodes and the slave node in a direction normal to the master surface.

- Adjust the volumes (optional) of the slave elements which have a master node located between the two slave nodes of the slave element.

This technique is illustrated in Figure 3. It can be seen that slave node s travels from A (at time = t - Δt) to B (at time = t) using the equations of motion from subsection 2.5. Since the velocity is constant for each time increment, the node travels in a straight line as shown. The master surface is also shown for time = t, and it can be seen that slave node s, at position B, has passed through the line connecting master nodes i and j. The slave node is next moved to position C, which is on the master surface. The line from B to C is normal to the master surface and therefore affects the equations of motion only in this normal direction. This also has the effect of assuming a frictionless surface.

18
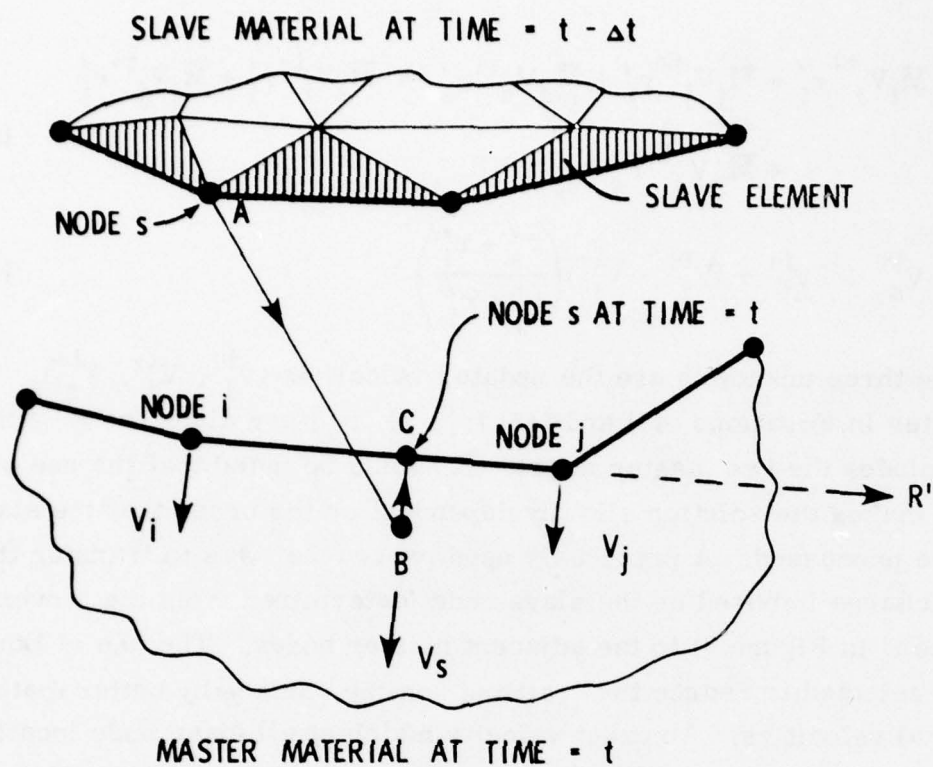
Figure 3. Sliding Surface Procedure

The next step consists of updating the normal velocities (V_i, V_j, V_s) of the three nodes. Since three unknowns are involved, three conditions must be specified to obtain a solution. Two of these conditions are that the translational and rotational momenta of the three nodes should be conserved. The third condition is that the normal velocity of the slave node is equal to the normal velocity of the master surface at the location of the slave node. The resulting three equations are

$$\overline{M}_i V_i^{t+} + \overline{M}_j V_j^{t+} + \overline{M}_s V_s^{t+} = \overline{M}_i V_i^{t-} + \overline{M}_j V_j^{t-} + \overline{M}_s V_s^{t-} \qquad (43)$$

19

$$\overline{M}_i V_i^{t+} r_i' + \overline{M}_j V_j^{t+} r_j' + \overline{M}_s V_s^{t+} r_s' = \overline{M}_i V_i^{t-} r_i' + \overline{M}_j V_j^{t-} r_j'$$
$$+ \overline{M}_s V_s^{t-} r_s' \tag{44}$$

$$V_s^{t+} = V_i^{t+} + (V_j^{t+} - V_i^{t+})\left(\frac{r_s' - r_i'}{r_j' - r_i'}\right) \tag{45}$$

where the three unknowns are the updated velocities (V_i^{t+}, V_j^{t+}, V_s^{t+}). The coordinates in Equations (44) and (45) (r_i', r_j', r_s') are along the R' axis which includes the two master nodes. It should be noted that the use of Equation (45) makes the solution slightly dependent on the order that the slave nodes are processed. A previously used procedure[7] was to transfer the momentum change imposed on the slave node (determined from the movement from B to C in Figure 3) to the adjacent master nodes. The use of Equation (45) was selected to reduce the "rattling" on the surface by better matching the normal velocities. An exact velocity match at all slave node locations could be obtained by repeatedly applying Equations (43) to (45) until the V^{t+} velocities were equal to the V^{t-} velocities. This would eliminate any order dependency. It should be emphasized that the order dependency is very minimal since the net momenta are conserved for the two master nodes and the slave node. It should also be noted that small errors are introduced into the center of gravity (cg) positions when the slave node is moved to the master surface, since there is no corresponding movement of the master nodes, which receive only instantaneous velocity changes. The cg errors are very small, however, and do not significantly affect the solutions.

2.7 SEVERE DISTORTIONS

A characteristic of a triangular formulation is that it is better suited to represent severe distortions than is a quadrilateral formulation. This is due to a triangle's resistance to allowing a node to cross the opposite side of the

triangle during the high distortion. It is apparent that the cross-sectional area of a triangle approaches zero as a node approaches the opposite side of that triangle. Since the hydrostatic pressure of Equations (26) and (29) is inversely proportional to the volume of the element, as the volume approaches zero the pressure approaches infinity. As a result, there is a very large resistance to this mode of distortion and the triangle will not go through a zero volume configuration provided the time increment is properly controlled.

The quadrilateral formulation does not have this desirable characteristic. Figure 4 shows three quadrilateral configurations which have equal cross-sectional areas, A_o. Configuration A shows a rectangular cross-section with nodes i, j, m and p defining the initial geometry. Configuration B represents a deformed element with nodes j and m occupying the same position. A triangular element with two nodes occupying the same position would result in a zero cross-sectional area. For the quadrilateral element, however, nodes i and p can be displaced to allow the initial area to be retained. Configuration C shows overlapping nodes and the net area of the quadrilateral is equal to the difference of the two triangular cross sections. Even this configuration can exist with the initial area. When this type of distortion is achieved, however, the formulation generally breaks down and numerical instability often occurs. The deformations represented by Configurations B and C usually occur when the grid is highly distorted. These deformations are resisted by the deviator stresses, but the deviator stresses are limited by the strength of the material and do not provide the potential magnitude of resistance as does the hydrostatic pressure for the triangular elements.

21
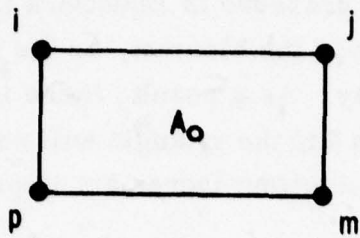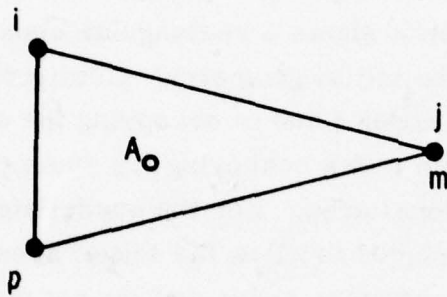
CONFIGURATION A

CONFIGURATION B
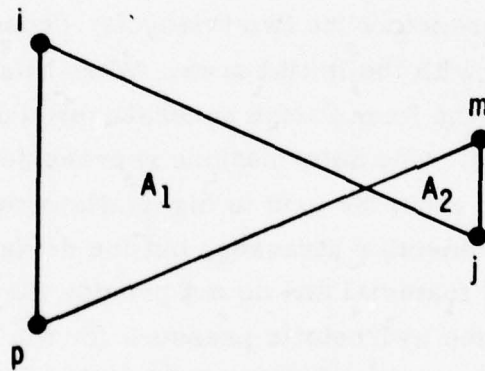
CONFIGURATION C

$$A_0 = A_1 - A_2$$

Figure 4. Possible Distortions of a Quadrilateral Element

2.8 BASIC VERIFICATION EXAMPLES

Several basic verification examples are included to illustrate and verify the computational technique. The first examples are shown in Figure 5 and they demonstrate the capability of the technique to provide accurate compressive wave propagation solutions. Figure 5a shows a radially restrained column of water impacting a rigid wall at 300m/s (Mach 0.2). Even though this reduces to a one-dimensional problem it is a severe test since the water is significantly compressed and the shock velocity is a function of the impact velocity, and therefore higher than the acoustic velocity. The dimensionless pressure is defined as $P^* = P/\rho_o C_o V_o$, where P, ρ_o, C_o and V_o represent the pressure, initial density, acoustic velocity and impact velocity, respectively. The pressure is shown at a time shortly before the wave reaches the far end of the column. It can be seen that the finite element solution with artificial viscosity agrees with the analytic solution along the length of the column, with only slight differences occurring at the leading edge of the wave. The solution obtained without artificial viscosity is also shown and it can be seen that the pressure radically oscillates about the analytic solution.

A similar example is shown in Figure 5b where a wave propagation solution is demonstrated for a detonated explosive. Here the dimensionless pressure is defined as $P^* = P/[\rho_o D^2/(\gamma +1)]$ where P, ρ_o and D are the pressure, initial density and detonation velocity, respectively, and γ is a material-dependent constant. Again it can be seen that there is excellent agreement between the finite element and analytic solutions.

Another compressive wave propagation example is shown in Figure 6. This example shows the effect of material strength with a higher-velocity elastic wave at the leading edge of the shock front and the elastic unloading at the rear. This solution is in good general agreement with that presented in Reference 1.

23

IMPACT EXAMPLE

COLUMN OF WATER WITH RADIAL RESTRAINT

RIGID BOUNDARY

FINITE ELEMENT MODEL

INITIAL GEOMETRY AT IMPACT OF $V_0 = 300$ M/S

DISPLACED GEOMETRY AT $\frac{C_0 t}{L} = 0.58$

$\frac{P}{\rho_0 C_0 V_0}$

DIMENSIONLESS PRESSURE

—————— ANALYTIC SOLUTION

●●●●● FINITE ELEMENT SOLUTION WITH ARTIFICIAL VISCOSITY

○○○○○ FINITE ELEMENT SOLUTION WITHOUT ARTIFICIAL VISCOSITY

(5a)

EXPLOSIVE DETONATION EXAMPLE

COLUMN OF EXPLOSIVE WITH RADIAL RESTRAINT

DETONATION INITIATED AT RIGID BOUNDARY

INITIAL GEOMETRY AT DETONATION

DISPLACED GEOMETRY AT $\frac{Dt}{L} = 0.95$

$\frac{P}{\frac{\rho_0 D^2}{\gamma + 1}}$

DIMENSIONLESS PRESSURE

0.5

0   0.2L   0.4L   0.6L   0.8L   1.0L

DISTANCE FROM RIGID BOUNDARY

(5b)

Figure 5. Wave Propagation Due to Impact and Explosive Detonation

24
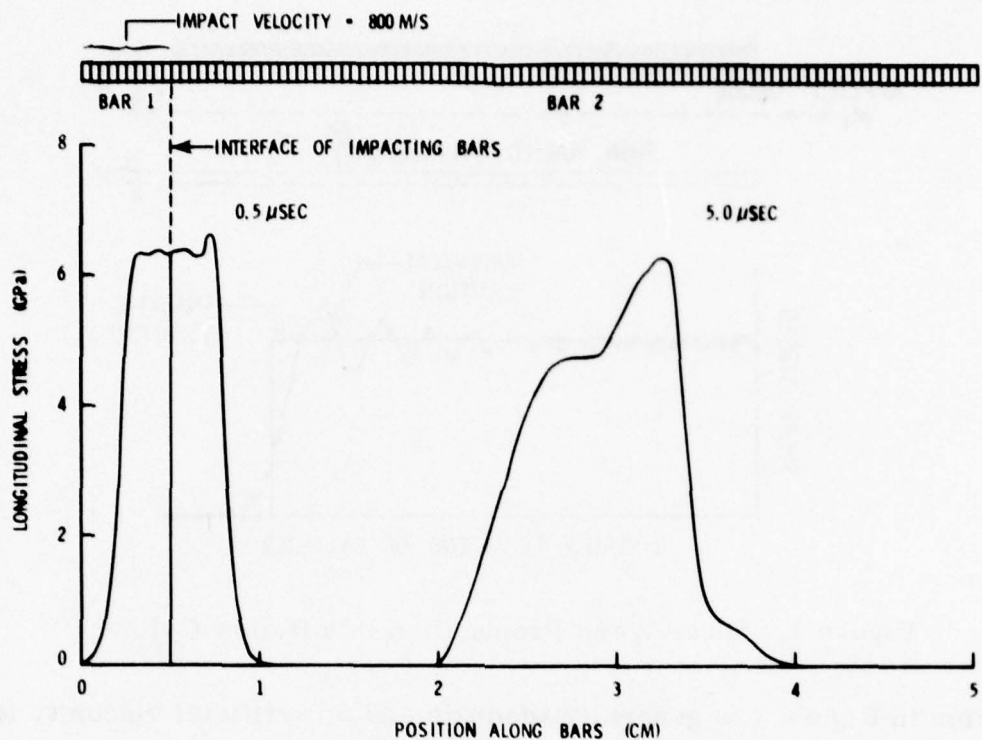
Figure 6. Wave Propagation Resulting From the Impact of two Bars

The capability to provide shear wave propagation solutions is shown in Figure 7 where a torque is suddenly applied to the end of a thin-walled cylinder. It can be seen that there is good general agreement between the two solutions, although the EPIC-2 solution does oscillate about the analytic solution. These oscillations exist because there is no artificial viscosity for the shear mode of deformation. The previously defined artificial viscosity in Equation (31) is affected only by volumetric strain rates. The need for artificial viscosity in the shear mode is not as critical as for the compressive mode, however. This is because the magnitude of the shear stress is bour led by the strength of the material whereas there is no upper bound for the magnitude of compressive waves. With the unbounded compressive stress it can be seen in Figure 5a that very radical oscillations can occur if the artificial viscosity is omitted. Since these radial oscillations cannot occur in the shear mode, due to the limitation on the strength of the material, the accuracy of the

25

APPLIED TORQUE
M_t

R

THIN WALLED CYLINDER $\left(\frac{R}{H} \cdot 10\right)$

H

NUMERICAL SOLUTION

ANALYTIC SOLUTION

SHEAR STRESS

DISTANCE FROM END OF CYLINDER
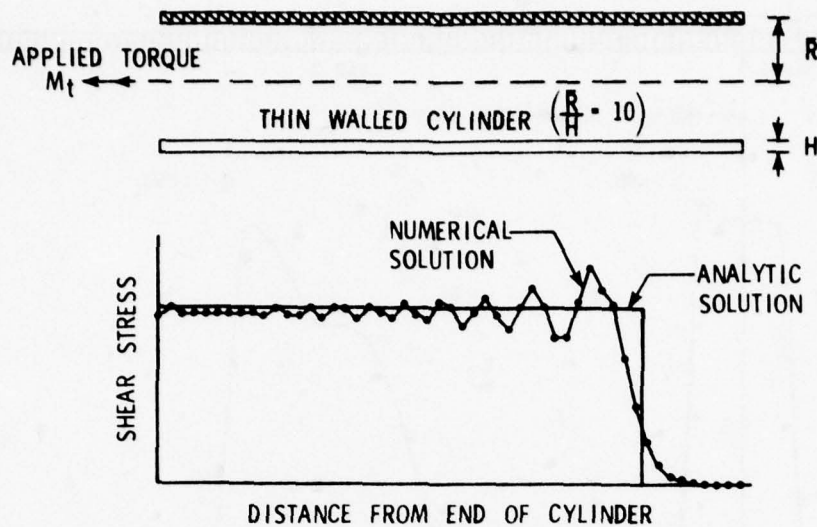
Figure 7.   Shear Wave Propagation in a Hollow Cylinder

solution in Figure 7 is generally adequate and no artificial viscosity is included for the shear mode of deformation.

A characteristic of spinning bodies is that transient dynamic responses are introduced if the spin is suddenly applied.   This can be illustrated by considering the case of a hoop subjected to a suddenly applied spin.   It can be shown that the radial stiffness of a ring is $K = 2 \pi AE/R_o$ and the mass is $M = 2 \pi R_o A\rho$ where A is the cross-sectional area, E is the modulus of elasticity, R_o is the radius and ρ is the density.   The period of vibration then becomes $T = 2\pi\sqrt{M/K} = 2\pi R_o/c_s$ where $c_s = \sqrt{E/\rho}$ is the sound velocity.   Figure 8 shows the response of a ring subjected to a suddenly applied spin ω.   For this problem the hoop is represented by three nodes and one triangular element.   It can be seen that the undamped spinning hoop behaves like a single-degree-of-freedom oscillator subjected to a suddenly applied force.   The response is plotted as dimensionless stress as a function of dimensionless time.   For the case of the spinning hoop the dimensionless stress is the ratio of the dynamic stress to the steady-state stress.   Likewise, the dimensionless time is the ratio of elapsed time to the period of vibration of the spinning

26

hoop. Both the magnitude of the response and the period of vibration are identical to those of a single-degree-of-freedom oscillator.
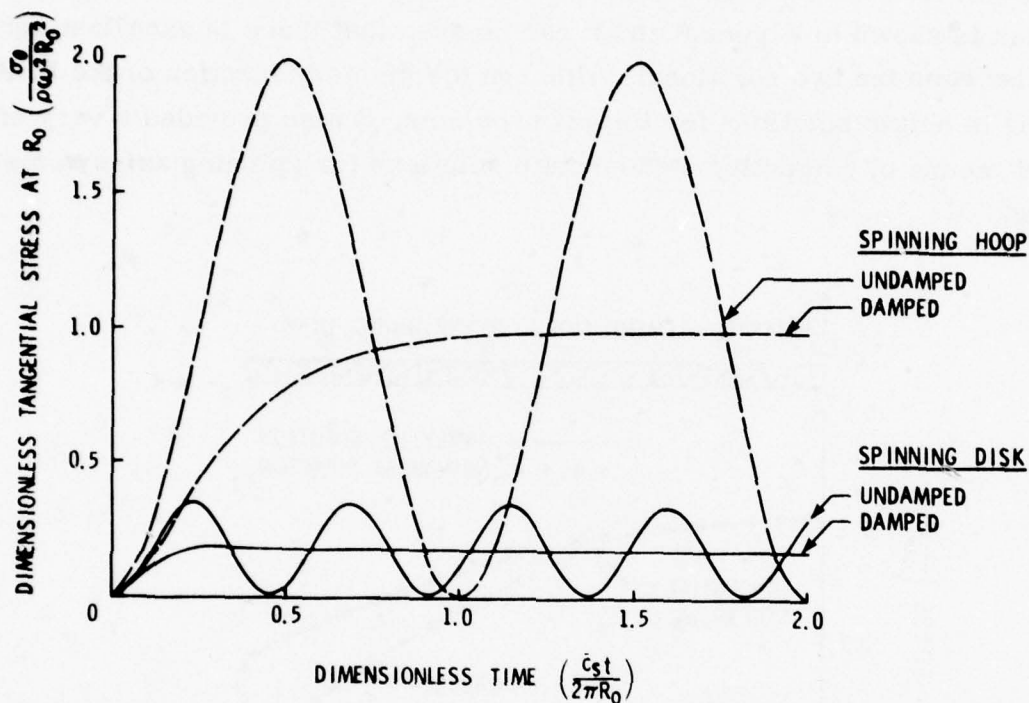
Figure 8. Dynamic Response of a Spinning Hoop and a Spinning Disk Subjected to a Suddenly Applied Spin

Since a spinning projectile probably attains a steady-state condition prior to striking the target, it is desirable to represent this steady-state condition with the computer simulation. This can be done by assuming the system is critically damped until a steady-state condition is achieved. Referring again to a single-degree-of-free system, the critical damping coefficient is $C_{CRIT} = 2Mc_s/R_o$. Since the resulting radial force is $F_{CRIT} = -C_{CRIT} \dot{R}$, the resulting velocity change during a time increment is $\Delta \dot{R} = F_{CRIT} \Delta t/M = -2c_s \Delta t \dot{R}/R_o$. This provides the basis for the damping effect in Equation (38) where the constant C_D is set equal to twice the sound velocity $(2c_s)$.

27

The response of a spinning disk is also shown in Figure 8. The basic response is similar to that of the hoop except both the period of vibration and the magnitude of the stress are much lower. The state of stress throughout the disk is shown in Figure 9 and it can be seen that there is excellent agreement between the two solutions. Although the primary function of the EPIC-2 code is to obtain solutions for impact problems, it also provides a very efficient means of computing steady-state solutions for spinning axi-symmetric bodies.
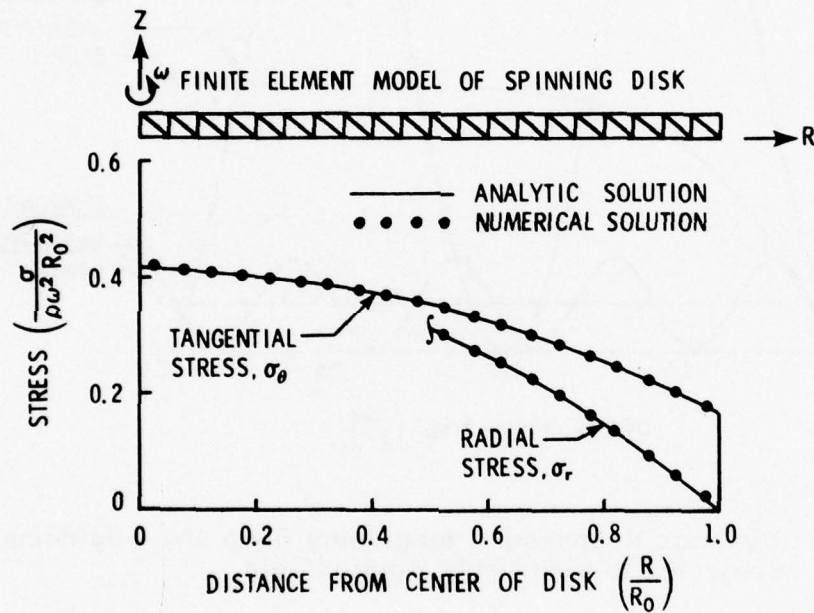
Figure 9. Stress Distribution in a Spinning Disk

This completes the discussion of the basic verification examples. Input data for a more comprehensive example is provided in the Appendix.

28

SECTION 3
COMPUTER PROGRAM DESCRIPTION

The EPIC-2 computer program contains the formulation presented in Section
2. A description of some of the characteristics of the computer program
is given in the following subsections.

3.1 PROGRAM ORGANIZATION AND SUBROUTINES

The organization of the EPIC-2 code is shown in the hierarchy chart in Figure
10. It consists of the main program, EPIC-2, and 18 subroutines for a total
of 3140 cards. The EPIC-2 code is core contained and requires 76K storage
on a Honeywell 6080 computer for a capacity of 1000 nodes and 2000 elements.
Two plotting programs are also available to provide state plots (geometry,
stress, strain, pressure and velocity fields) at specific times, and to plot
various system parameters (energy, momentum, etc.) as functions of time.
The following is a brief description of the main program and subroutines
(listed alphabetically) shown in Figure 10.

EPIC-2   This is the main program which calls subroutines HDATA,
              MATL, GEOM, START and LOOP (77 cards)

BREAK   This subroutine checks for fracture (21 cards)

ELEG   This subroutine generates a series of triangular elements (61
              cards)

ESHAPE   This subroutine generates elements for special shapes includ-
              ing rods with various nose shapes, spheres and plates (236
              cards)

29
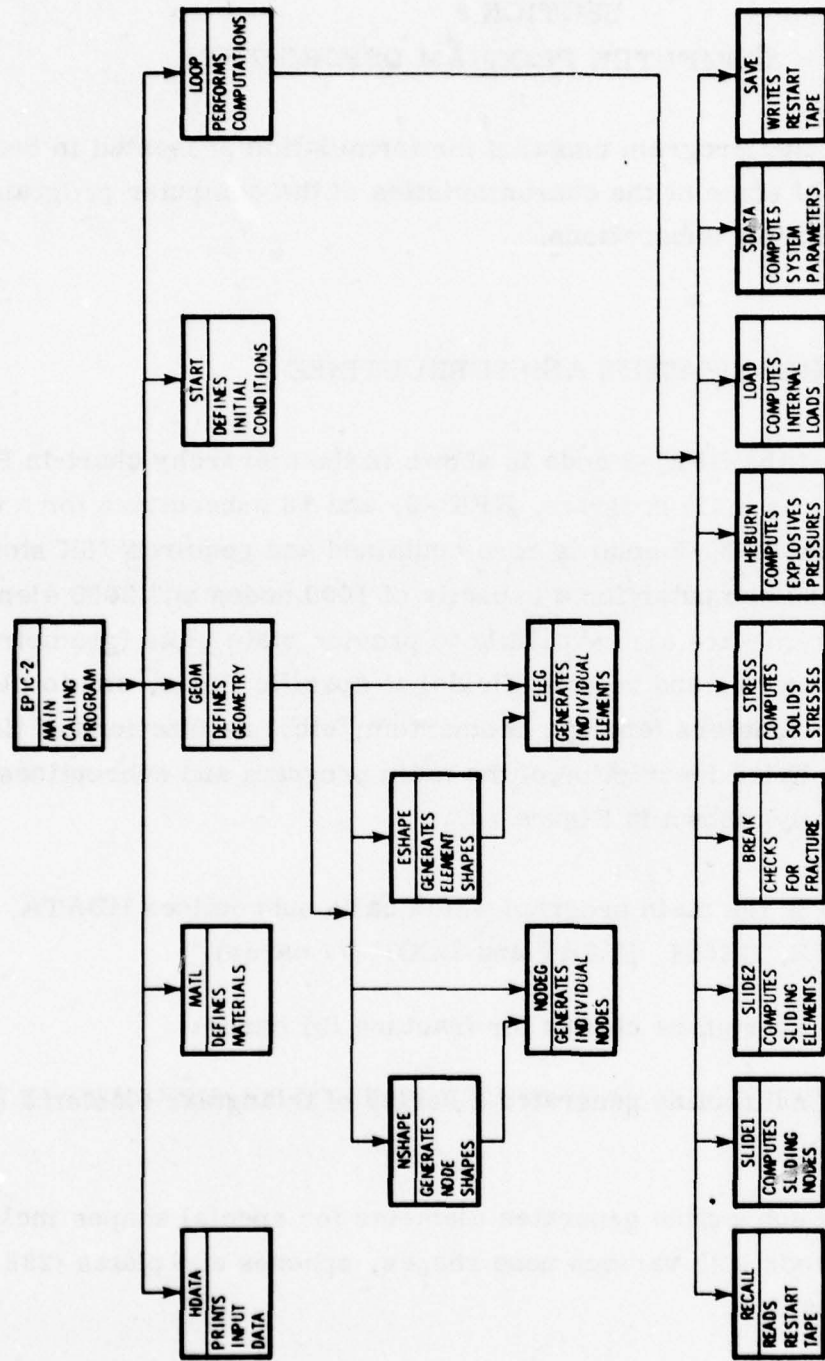
Figure 10. Hierarchy Chart for the EPIC-2 Main Program

GEOM   This subroutine reads, generates and prints the initial geometry (438 cards)

HDATA   This subroutine prints all data as it is input (29 cards)

HEBURN   This subroutine computes pressures and energies for explosive elements (58 cards)

LOAD   This subroutine computes internal axial and torsional loads in an axi-symmetric rod (41 cards)

LOOP   This subroutine computes the equations of motion, strains, strain rates, stresses, pressures and concentrated nodal forces. It also prints selected node and element data (498 cards)

MATL   This subroutine reads and prints material data (189 cards)

NODEG   This subroutine generates a row of nodes (64 cards)

NSHAPE   This subroutine generates nodes for special shapes including rods with various nose shapes, spheres and plates (220 cards)

RECALL   This subroutine reads data from Tape 2 for a restart run (93 cards)

SAVE   This subroutine writes data on Tape 2 for a restart run or a state plot (89 cards)

SDATA   This subroutine computes system data such as energy, momentum, etc., for the projectile, target and total system. It also writes this data on Tape 3 for time plots (157 cards)

SLIDE1   This subroutine computes the equations of motion for the slave nodes. If there is interference with the master surface, it

places the slave node on the master surface and redistributes the momenta of the slave and master nodes (411 cards)

SLIDE2   This subroutine computes the cross-sectional area and volume change to the slave elements caused by the master surface intruding into the elements (158 cards)

START   This subroutine reads the initial dynamic or detonation conditions and sets the variables equal to the conditions which exist at impact and/or explosive detonation (145 cards)

STRESS   This subroutine computes stresses and energies for the solid-liquid elements. The stresses consist of elastic, plastic and viscous stresses, hydrostatic pressure and artificial viscosity (155 cards)

The plotting program for state plots reads data from Tape 2 and generates plots for geometry, stress, strain, pressure and velocity fields at specified times. The plotting program for time plots reads data from Tape 3 and generates time-dependent plots for the following system parameters: center of gravity, kinetic energy, internal energy, total energy, plastic work, axial momentum, axial velocity, spin momentum, spin velocity, maximum axial coordinate and minimum axial coordinate. Each plot presents data for the projectile, target and total system.

3.2 NODE AND ELEMENT ARRAYS

There are 13 node variables which are contained in common arrays and 19 element variables contained in common arrays. The node arrays are described as follows:

32

R	The radial R coordinate of the node (see Figure 2)
Z	The axial Z coordinate of the node
T	The angular θ coordinate of the node
RDOT	The radial velocity of the node
ZDOT	The axial velocity of the node
TDOT	The angular velocity of the node
FR	The radial force acting on the node
FZ	The axial force acting on the node
FT	The circumferential force acting on the node
NODE	Identifies the node number such that it is not necessary to have a consecutive node numbering system. The node number must not be greater than the dimension of the node arrays, however.
AMASS	The total mass of the node
PMASS	The mass of the node contributed by the projectile
IRZT	Identifies radial, axial and circumferential restraints on the node. It also identifies a slave node and indicates if it is free or sliding on the master surface

The element arrays are described as follows:

NEL	Identifies the element number. Must not be greater than the dimension of the element arrays.

NODE1	Node number of node i (see Figure 2)
NODE2	Node number of node j
NODE3	Node number of node m
ICHECK	Identifies state of material (elastic, plastic, fractured)
SR	Total normal stress in the radial direction
SZ	Total normal stress in the axial direction
ST	Total normal stress in the circumferential direction
SRZ	Shear stress in the R-Z plane
SRT	Shear stress in the R-θ plane
SZT	Shear stress in the Z-θ plane
VOL	Initial volume of the element
DVOL	Volumetric strain
MAT	Material number
EBAR	Equivalent plastic strain defined in Equation (13)
ES	Total internal energy per original unit volume defined in Equation (27)
DAREA	The cross-sectional area of the master surface intruding into a slave element
DDVOL	The volume of the master surface intruding into a slave element
TSTART	The time required for the detonation wave to arrive at the nearest node of the element from the point of detonation.

34

SECTION 4
PROGRAM USER INSTRUCTIONS

The required EPIC-2 input data for various conditions are summarized in Figure 11 and described in subsections 4.1 through 4.4. Output data are described in subsection 4.5. Succeeding subsections deal with diagnostics, estimated central processor time requirements, and central memory storage requirements and alterations.

4.1 INPUT DATA FOR AN INITIAL RUN

An initial run is one which requires input data for the initial geometry and impact/detonation conditions at time = 0. The descriptions which follow are for the input data in Figure 11. Consistent units must be used.

Identification Card (4I5, F10.0)

CASE   = Case number for run identification

CYCLE = 0 for initial run

IMAT   = A code describing the types of materials. Two options are available.

      IMAT = 1 reads material properties for solid-liquid elements. (no explosive element data read)

      IMAT = 2 reads material properties for solid-liquid elements and explosive elements.

INITIAL RUN INPUT DATA

IDENTIFICATION CARD (4I5, F10.0)

CASE	CYCLE	IMAT	GEOM	CPMAX	

23 SOLID-LIQUID MATERIAL CARDS (5E15.8)

MATL1	MATL2	MATL3	MATL4	MATL5	

6 EXPLOSIVE MATERIAL CARDS - FOR IMAT = 2 (5E15.8)

MATL6	MATL7	MATL8	MATL9	MATL10	

MISCELLANEOUS CARD (7I5)

NSLID	IRIG	NMASS	NDEP	NTOP	NBOT	NRING	

PROJECTILE SCALE / SHIFT / ROTATE CARD (5F10.0)

RSCALE	ZSCALE	ROTATE	RSHIFT	ZSHIFT	

PROJECTILE NODE DATA CARDS - AS REQUIRED (3I5, 2X, 3I1, 5F10.0)

N1	NN	INC				R1	Z1	RN	ZN	EXPAND	

└─ IR, IZ, IT

BLANK CARD

PROJECTILE NODE SPECIAL SHAPES - AS REQUIRED (DESCRIPTION FOLLOWS)

BLANK CARD

TARGET SCALE / SHIFT / ROTATE CARD (5F10.0)

RSCALE	ZSCALE	ROTATE	RSHIFT	ZSHIFT	

TARGET NODE DATA CARDS - AS REQUIRED (3I5, 2X, 3I1, 5F10.0)

N1	NN	INC				R1	Z1	RN	ZN	EXPAND	

└─ IR, IZ, IT

BLANK CARD

TARGET NODE SPECIAL SHAPES - AS REQUIRED (DESCRIPTION FOLLOWS)

BLANK CARD

PROJECTILE ELEMENT DATA CARDS - AS REQUIRED (9I5)

ELE1	ELEN	ELE INC	MATL	N1	N2	N3	N4	NODE INC	

BLANK CARD

PROJECTILE ELEMENT SPECIAL SHAPES - AS REQUIRED (DESCRIPTION FOLLOWS)

BLANK CARD

TARGET ELEMENT DATA CARDS - AS REQUIRED (9I5)

ELE1	ELEN	ELE INC	MATL	N1	N2	N3	N4	NODE INC	

BLANK CARD

Figure 11. Summary of Input Data

36

TARGET ELEMENT SPECIAL SHAPES - AS REQUIRED (DESCRIPTION FOLLOWS)

BLANK CARD

CONCENTRATED MASS CARDS - AS REQUIRED (I5, E15.8)

N	MASS (N)	

RIGID BODY IDENTIFICATION CARDS - AS REQUIRED (I5)

NDN	

RIGID BODY NODES - AS REQUIRED (15I5)

ID1	ID2													ID15	

SLIDING SURFACE IDENTIFICATION CARDS - AS REQUIRED (3I5)

NMN	NSN	NSE	

MASTER NODES - AS REQUIRED (16I5)

IM1	IM2													IM15	IM16

SLAVE NODES - AS REQUIRED (16I5)

IS1	IS2													IS15	IS16

SLAVE ELEMENTS - AS REQUIRED (16I5)

ISE1	ISE2													ISE15	ISE16

INITIAL VELOCITY / DETONATION CARD (8F10.0)

PRDOT	PZDOT	PTDOT	TRDOT	TZDOT	TTDOT	RDET	ZDET

INTEGRATION TIME INCREMENT CARD (6F10.0)

DT1	DTMAX	DTMIN	SSF	TMAX	TBURN	

DATA OUTPUT CARDS - AS REQUIRED (4F10.0, 3I5)

TIME	ECHECK	BCHECK	RDAMP	ILOAD	ISAVE	IDATA	

RESTART RUN INPUT DATA

IDENTIFICATION CARD (3I5, 5X, F10.0)

CASE	CYCLE	IWIND		CPMAX	

INTEGRATION TIME INCREMENT CARD (3F10.0)

DTMIN	SSF	TMAX	

DATA OUTPUT CARDS - AS REQUIRED (4F10.0, 3I5)

TIME	ECHECK	BCHECK	RDAMP	ILOAD	ISAVE	IDATA	

Figure 11.   Summary of Input Data (Continued)

SPECIAL SHAPES INPUT DATA FOR NODES

IDENTIFICATION CARD FOR ROD NODES (4I5, 3F10.0)

1	N1	NRING	NPLN	ZTOP	ZBOT	EXPAND	

TOP RADII CARD(S) FOR ROD NODES (8F10.0)

RT(1)	RT(2)					RT(NRING)	

BOTTOM RADII CARD(S) FOR ROD NODES (8F10.0)

RB(1)	RB(2)					RB(NRING)	

IDENTIFICATION CARD FOR NOSE NODES (3I5, 5X, F10.0)

INOSE	N1	NRING		ZTOP	

TOP RADII CARD(S) FOR NOSE NODES (8F10.0)

RT(1)	RT(2)					RT(NRING)	

MINIMUM Z COORDINATE CARD(S) FOR NOSE NODES (8F10.0)

ZM(1)	ZM(2)					ZM(NRING)	

CARD FOR SPHERE NODES (3I5, 5X, 2F10.0)

4	N1	NRING		ZTOP	ZBOT	

IDENTIFICATION CARD FOR FLAT PLATE NODES (2I5)

5	N1	

DESCRIPTION CARD FOR FLAT PLATE NODES (4I5, 6F10.0)

NR	NZ	IDZ	IRFIX	RMAX	RMIN	ZMAX	ZMIN	R-EXPAND	Z-EXPAND

SPECIAL SHAPES INPUT DATA FOR ELEMENTS

IDENTIFICATION CARD FOR ROD ELEMENTS (6I5)

1	N1	NRCOL	NZLAY	IDIA	ELE1	

MATERIAL CARD FOR ROD ELEMENTS (15I5)

M(1)	M(2)					M(NRCOL)								

IDENTIFICATION CARD FOR NOSE ELEMENTS (3I5, 10X, I5)

INOSE	N1	NRING		ELE1	

MATERIAL CARD FOR NOSE ELEMENTS (15I5)

M(1)	M(2)					M(NRCOL)								

CARD FOR SPHERE ELEMENTS (3I5, 10X, 2I5)

4	N1	NRING		ELE1	MATL	

CARD FOR FLAT PLATE ELEMENTS (7I5)

5	N1	NRLAY	NZLAY	IDIA	ELE1	MATL	

Figure 11.   Summary of Input Data (Continued)

STATE PLOTS INPUT DATA

STATE PLOT IDENTIFICATION CARDS - AS REQUIRED (2I5, 4F10.0)

TYPE	CYCLE	ZMAX	ZMIN	RMAX	RMIN	

DEFORMED GEOMETRY PLOT CARD - FOR TYPE = 1 (3A6, 2X, 4I5)

TITLE		EDGE	IE	IP	IF	

STRESS FIELD PLOT CARD - FOR TYPE = 2 (3A6, 2X, 2I5, 5F10.0)

TITLE		EDGE	NLINE	STRESS(1)	STRESS(2)	STRESS(3)	STRESS(4)	STRESS(5)

PRESSURE FIELD PLOT CARD - FOR TYPE = 3 (3A6, 2X, 2I5, 5F10.0)

TITLE		EDGE	NLINE	PRES(1)	PRES(2)	PRES(3)	PRES(4)	PRES(5)

STRAIN FIELD PLOT CARD - FOR TYPE = 4 (3A6, 2X, 2I5, 5F10.0)

TITLE		EDGE	NLINE	STRAIN(1)	STRAIN(2)	STRAIN(3)	STRAIN(4)	STRAIN(5)

VELOCITY FIELD PLOT CARD - FOR TYPE = 5 (3A6, 2X, I5, 5X, F10.0)

TITLE		EDGE		VSCALE	

BLANK CARD	ENDS RUN

TIME PLOTS INPUT DATA

TIME PLOT DESCRIPTION CARDS - AS REQUIRED (I5, 5X, 4F10.0, 4A6)

TYPE		TMAX	TMIN	VMAX	VMIN	TITLE	

TYPE		VARIABLE PLOTTED
1	-	CENTER OF GRAVITY
2	-	KINETIC ENERGY
3	-	INTERNAL ENERGY
4	-	TOTAL ENERGY
5	-	PLASTIC WORK
6	-	AXIAL MOMENTUM
7	-	AXIAL VELOCITY
8	-	SPIN MOMENTUM (R MOMENTUM FOR PLANE STRAIN)
9	-	SPIN VELOCITY (R VELOCITY FOR PLANE STRAIN)
10	-	MAXIMUM AXIAL COORDINATE
11	-	MINIMUM AXIAL COORDINATE

BLANK CARD	ENDS RUN

Figure 11. Summary of Input Data (Concluded)

IGEOM   = A code describing the geometry of the problem

              IGEOM = 1 defines axi-symmetric geometry

              IGEOM = 2 defines plane strain geometry

CPMAX = Central processor time (hours) at which the results will be written on the restart and plot tape (if previously requested) and the run will stop. This feature will be bypassed if CPMAX = 0.

23 Material Cards for Solids and Liquids (5E15. 8)

These cards are included for IMAT = 1 or IMAT = 2. Each of the 23 material cards provides a specific material characteristic for five materials. For instance, the first card describes the density of the materials. The density of material 1 is entered in columns 1-15, the density of material 2 in columns 16-30, etc. The second card contains the specific heats for the five materials, etc. It is only necessary to describe the materials used for the analysis. If materials 1 and 3 are used for a specific analysis, all the material 1 data must be specified in columns 1-15 and all the material 3 data in columns 31-45. Columns 16-30, 46-60, and 61-75, representing materials 2, 4 and 5, can be left blank.

Card 1   Density (mass/volume)

Card 2   Specific heat (work/mass/degree)

Card 3   Shear modulus of elasticity (force/area)

Card 4   Absolute viscosity for Navier-Stokes Equations (force-time/area)

Card 5   Yield stress (force/area)

Card 6   *Ultimate stress (force/area)*

40

Card 7   Strain at which the ultimate stress is achieved. Should be consist-
          ent with the equivalent plastic strain definition in Equation (13)
          which is essentially a "true" strain. Stress varies linearly between
          the yield stress and the ultimate stress. The stress for larger
          strains is equal to the ultimate stress until fracture occurs.

Card 8   Maximum negative hydrostatic pressure (force/area)

Card 9   Strain rate effect constant, C_1, in Equation (24)

Card 10   Pressure effect constant, C_2, in Equation (24)

Card 11   Pressure effect constant, C_3, in Equation (24)

Card 12   Temperature effect constant, C_4, in Equation (24)

Card 13   Temperature effect constant, C_5, in Equation (24)

Card 14   Hydrostatic pressure constant, K_1, in Equation (26) (force/area)

Card 15   Hydrostatic pressure constant, K_2, in Equation (26) (force/area)

Card 16   Hydrostatic pressure constant, K_3, in Equation (26) (force/area)

Card 17   Grüneisen coefficient, Γ, in Equation (26)

Card 18   Linear artificial viscosity coefficient, C_L, in Equation (31)

Card 19   Quadratic artificial viscosity coefficient, $C_o{}^2$, in Equation (31)

Card 20 ⎫ Equivalent strain ⎫ If either is exceeded there is a shear and
Card 21 ⎭ Volumetric strain ⎭ tensile failure. Positive hydrostatic pres-
                               sure and viscosity stress capability remain.
                               If Equivalent strain is negative; material
                               behaves like a liquid.

Card 22   Equivalent strain   If exceeded the element fails totally and
                               produces no stresses or pressures.

Card 23   Initial temperature (degrees)

<u>Six Material Cards for Explosives (5E15. 8)</u>

These cards are included only if IMAT = 2 in the Identification Card. The explosive material numbers are designated 6 through 10 with material 6 entered in columns 1-15, etc.

Card 1   Density (mass/volume)

Card 2   Internal Energy. Initial value of E_s in Equation (29) (energy/volume)

Card 3   Detonation velocity (distance/time)

Card 4   Material constant, γ, in Equation (29)

Card 5   Linear artificial viscosity coefficient, C_L, in Equation (31)

Card 6   Quadratic artificial viscosity coefficient, C_o^2, in Equation (31)

<u>Miscellaneous Card (7I5)</u>

NSLID   =   The number of sliding surfaces (currently limited to a max-
                   imum of five). This does not include the rigid sliding sur-
                   face which follows.

IRIG   =   1 gives a rigid frictionless surface on the positive side of the
                   plane described by $Z = 0$. If the equations of motion cause a
                   node to have a negative Z coordinate, the node coordinate is
                   redefined and set to $Z = 0$. If IRIG = 0 this option is not used.

NMASS   =   The number of concentrated masses to be entered later. These
                   masses are in addition to the concentrated masses automatic-
                   ally generated from the elements.

NDEP   =   The number of systems of nodes which are designated to travel
                   as a rigid body in the axial direction. It does not apply to the
                   radial velocities. The specific nodes are input later.

42

The next three variables (NTOP, NBOT, NRING) are used to identify the nodal geometry for internal load calculations in a slender projectile with axi-symmetric geometry (IGEOM = 1). If this option is used, the nodal geometry must be consistent with the arrangement of nodes generated by *the special shapes generator for rod geometry. Leave blank if it will not be used.*

NTOP = The node number of the centerline node at the **top free end** of the cylindrical projectile.

NBOT = The node number of the centerline node at the lower end of the cylindrical portion of the projectile.

NRING = The number of rings of nodes in the cylindrical projectile. This will be described in the discussion of the special shapes.

Projectile Scale/Shift/Rotate Card (5F10. 0)

RSCALE = Factor by which the R coordinates of all projectile nodes are multiplied. Applied after the coordinate shifts (RSHIFT, ZSHIFT) and before the rotation (ROTATE) described later.

ZSCALE = Factor by which the Z coordinates are multiplied.

ROTATE = Rotation about R = Z = 0 in the R-Z plane of all projectile nodes (degrees). (Positive clockwise) Applied after the coordinate shifts (RSHIFT, ZSHIFT), and the scale factors (XSCALE, ZSCALE).

RSHIFT = Increment added to the R coordinates of all projectile nodes (length). Applied before the scale factors (RSCALE, ZSCALE).

ZSHIFT = Increment added to the Z coordinates (length).

43

Projectile Node Data Cards (3I5, 2X, 3I1, 5F10. 0)

The Projectile Node Data Cards are provided as required for the projectile nodes. If a node is at the interface of the projectile and the target and contains mass from both the projectile and the target, it must be included with the projectile nodes. The node numbers (N1 • • • NN) must not exceed the dimension of the node arrays, and they need not be numbered consecutively or in increasing order. End with a blank card.

N1 = First node in a row of nodes.

NN = Last node in a row of nodes. Leave blank if a single node (not a row) is entered.

INC = Node number increment between adjacent nodes. If left blank, program will set INC = 1.

IR = 1 will restrain all nodes (N1 · · · NN) in the radial R direction. No restraint if left blank.

IZ = 1 will restrain nodes in the axial Z direction

IT = 1 will restrain nodes in the circumferential θ direction

R1 = Radial coordinate of node N1 (length)

Z1 = Axial coordinate of node N1 (length)

RN = Radia coordinate of node NN (length). Leave blank if a single node is entered.

ZN = Axial coordinate of node NN (length)

EXPAND = Factor by which the distance between adjacent nodes changes. For example, if the distance between the first two nodes is Δ_1, the distance between the second and third nodes is $\Delta_2 = \Delta_1$. EXPAND. A summary of relative spacing between the

44

first two nodes and the last two nodes is given in Figure 12.
Analytic expressions are also provided for cases not included
in the Figure. If left blank, the program will set EXPAND =
1.0 for uniform spacing.

NUMBER OF INCRE- MENTS N	EXPAND																	
	.7		.8		.9		1.0		1.1		1.2		1.3		1.4		1.5	
	$\frac{\Delta_1}{\bar\Delta}$	$\frac{\Delta_N}{\bar\Delta}$	$\frac{\Delta_1}{\bar\Delta}$	$\frac{\Delta_N}{\bar\Delta}$	$\frac{\Delta_1}{\bar\Delta}$	$\frac{\Delta_N}{\bar\Delta}$	$\frac{\Delta_1}{\bar\Delta}$	$\frac{\Delta_N}{\bar\Delta}$	$\frac{\Delta_1}{\bar\Delta}$	$\frac{\Delta_N}{\bar\Delta}$	$\frac{\Delta_1}{\bar\Delta}$	$\frac{\Delta_N}{\bar\Delta}$	$\frac{\Delta_1}{\bar\Delta}$	$\frac{\Delta_N}{\bar\Delta}$	$\frac{\Delta_1}{\bar\Delta}$	$\frac{\Delta_N}{\bar\Delta}$	$\frac{\Delta_1}{\bar\Delta}$	$\frac{\Delta_N}{\bar\Delta}$
2	1.176	.824	1.111	.889	1.053	.947	1.0	1.0	.952	1.048	.909	1.091	.870	1.130	.833	1.167	.800	1.200
3	1.370	.671	1.230	.787	1.107	.897			.906	1.097	.824	1.187	.752	1.271	.688	1.349	.632	1.421
4	1.579	.542	1.355	.694	1.163	.848			.862	1.147	.745	1.288	.647	1.420	.563	1.545	.492	1.662
5	1.803	.433	1.487	.609	1.221	.801			.819	1.199	.672	1.393	.553	1.579	.457	1.755	.379	1.919
6	2.040	.343	1.626	.533	1.281	.756			.778	1.252	.604	1.504	.470	1.746	.368	1.977	.289	2.192
7	2.288	.269	1.772	.464	1.342	.713			.738	1.307	.542	1.618	.398	1.922	.293	2.210	.218	2.487
8	2.547	.210	1.923	.403	1.405	.672			.700	1.363	.485	1.737	.335	2.104	.233	2.452	.162	2.775
9	2.814	.162	2.079	.349	1.469	.632			.663	1.421	.433	1.861	.281	2.293	.183	2.702	.120	3.080
10	3.087	.125	2.241	.301	1.535	.595			.627	1.479	.385	1.988	.235	2.488	.143	2.959	.088	3.392
12	3.651	.072	2.577	.221	1.672	.525			.561	1.601	.303	2.253	.161	2.893	.086	3.490	.047	4.031
14	4.229	.041	2.929	.161	1.815	.461			.500	1.728	.237	2.530	.109	3.315	.051	4.036	.024	4.683
16	4.816	.023	3.293	.116	1.964	.404			.445	1.859	.183	2.819	.073	3.749	.030	4.592	.012	5.341
18	5.409	.013	3.666	.083	2.118	.353			.395	1.995	.140	3.117	.048	4.191	.017	5.155	.006	6.004
20	6.003	.005	4.037	.046	2.246	.273			.312	2.102	.089	3.407	.024	4.634	.007	5.719	.002	6.668

NODES N1 (N1 + INC) (NN - INC) NN

INCREMENTS Δ_1 Δ_2 Δ_{I-1} Δ_I Δ_{I+1} Δ_{N-1} Δ_N

$$\bar\Delta = \frac{\text{TOTAL LENGTH}}{\text{NUMBER INCREMENTS}} = \frac{L}{N} \qquad\qquad \Delta_{I+1} = \Delta_I \cdot \text{EXPAND}$$

$$\frac{\Delta_1}{\bar\Delta} = \frac{N(1-\text{EXPAND})}{(1-\text{EXPAND}^N)} \qquad\qquad \frac{\Delta_N}{\bar\Delta} = \frac{N(1-\frac{1}{\text{EXPAND}})}{[1-(\frac{1}{\text{EXPAND}})^N]}$$
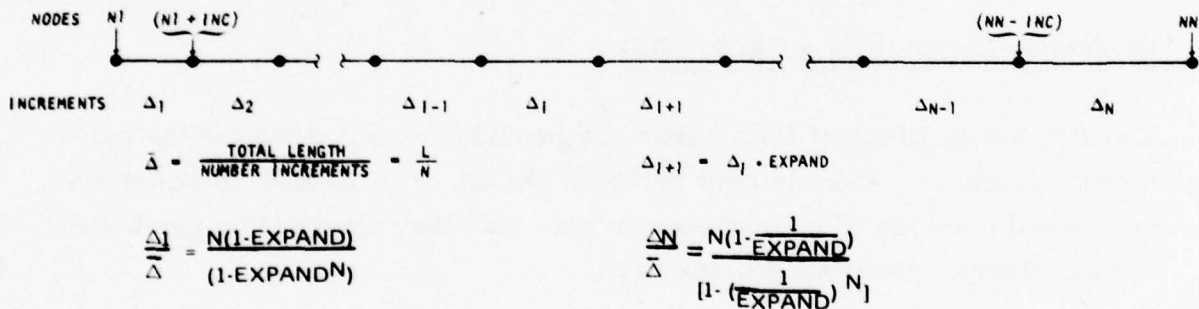
Figure 12. Nodal Spacing for Various Expansion Factors

Projectile Node Special Shapes

These are described later. End with a blank card.

Target/Scale/Shift/Rotate Card (5F10. 0)

Same as Projectile Scale/Shift/Rotate card except it applies to the target nodes.

Target Node Data Cards (3I5, 2X, 3I1, 5F10. 0)

Same as the Projectile Note Data cards. If there are interface nodes which contain mass from both the projectile and the target, these nodes are included with the projectile nodes and must not be included here. End with a blank card.

Target Node Special Shapes

These are defined later. End with a blank card.

Projectile Element Data Cards (9I5)

The Projectile Element Data cards are provided as required for the projectile elements. The element numbers (ELE1 · · · ELEN) must not exceed the dimension of the element arrays, and they need not be numbered consecutively. End with a blank card.

ELE1   = First individual element in a series of elements.

ELEN   = Last individual element in a series of elements. Must be greater than ELE1. Leave blank if a single element is entered.

ELE INC   = Element number increment between successive elements.
              If left blank, the program will set ELE INC = 1. (Example:
              If ELE1 = 100, ELEN = 104, and ELE INC = 2, there will
              be three elements designated at 100, 102, and 104).

MATL   = Material number (1-10) of the elements. If left blank, the
              material number from the previous element data card will
              be used.

N1 - N4   = Node numbers for the first composite element which contains
              two individual triangular elements. Nodes N1, N2 and N3
              (Counterclockwise) define the first element in the composite
              elements and nodes N1, N3 and N4 (counterclockwise) define
              the second element. If N4 is blank, the second element will
              not be generated.

NODE INC   = The node number increment added to the node numbers of
              the previous composite or individual element. If left blank,
              the program will set NODE INC = 1. (Example: If N1 - N4
              are 24, 20, 22 and 26 and if NODE INC = 4, then the nodes
              of the second composite element are 28, 24, 26, and 30).

Projectile Element Special Shapes

These are defined later. End with a blank card.

Target Element Data Cards (9I5)

Same as Projectile Element Data cards. End with a blank card.

47

Target Element Special Shapes

These are defined later.   End with a blank card.

Concentrated Mass Cards (I5, E15. 8)

There are NMASS (Defined in Miscellaneous card) cards entered for the concentrated masses.   Each card contains data for one mass.

N   = The node number to which the concentrated mass is added.

MASS(N) = The concentrated mass added to node N.

Rigid-Body Identification Cards (I5)

Each system of rigid-body nodes contains one Rigid-Body Identification card and one Rigid-Body Nodes card.   The program is dimensioned for a maximum of five rigid-body systems with a maximum 15 nodes per system. If there are no rigid-body systems (NDEP = 0 in Miscellaneous card) this group of cards is omitted.   If there is more than one system of rigid-body nodes, both cards for the system are entered before the Rigid-Body Identification card for the second system is entered.

NDN = The number of rigid-body nodes in this system.

Rigid-Body Nodes Card (15I5)

ID1, ID2, . . . are the node numbers for the rigid-body nodes which can be input in any order.   These nodes will always have identical velocities in the

Z direction. Master nodes (defined later) can be included but slave nodes (defined later) cannot be included.

Sliding Surface Identification Cards (3I5)

Each sliding surface contains one identification card and cards (as required) describing the master nodes, slave nodes and the slave elements. The program is dimensioned for a maximum of five sliding surfaces which can each contain a maximum of 100 master nodes, 100 slave nodes and 100 slave elements. If there are no sliding surfaces (NSLID = 0 on Miscellaneous card) this group of cards is omitted. If there is more than one sliding surface, all data for the first sliding surface are entered before the second Sliding Surface Identification card is entered.

NMN = The number of master nodes on the sliding surface

NSN = The number of slave nodes on the sliding surface

NSE = The number of slave elements on the sliding surface. A slave element is a triangular element which must contain two slave nodes. If an element is designated as a slave element, the cross-sectional area (and the resulting volume) will be adjusted if a master node is located between the two slave nodes. It is not necessary, however, to include slave elements to allow the problem to run.

Master Node Cards (16I5)

IM1, IM2, . . . are the node numbers of a row of master nodes. The nodes must be entered in order from the first master node to the last master node along the row of nodes. When moving from the first node to the last node, the slave nodes (and elements) must be to the left of the master surface.

Slave Node Cards (16I5)

IS1, IS2, . . . are the node numbers of the slave nodes. No special order is required. If there are no slave elements (NSE = 0) it is possible to designate interior nodes (as well as surface nodes) as slave nodes. This procedure allows elements containing **slave** nodes to fail completely to simulate the eroding process. The slave node spacing should not be significantly greater than the master node spacing or localized deformations in the master surface may occur. A slave node can be restrained only in the radial direction, and only if the radial coordinate of the slave node is equal to the radial coordinate of the first or last master node, which must also be restrained in the radial direction. This allows a slave node on the Z axis to be restrained.

Slave Element Cards (16I5)

ISE1, ISE2, . . . are the element numbers of the slave elements. If very severe distortions are expected on the slave surface, it may be desirable to not designate any slave elements since numerical instability problems may occur. If an element is designated as a slave element , the element must contain exactly two nodes which are slave nodes.

Initial-Velocity/Detonation Card (8F10.0)

This card describes the initial-velocity and/or detonation conditions. If there are interface nodes which include mass from both the projectile and the target, the velocities of these nodes are adjusted by the program to conserve momenta.

PRDOT = Projectile velocity in the R direction (distance/time)

PZDOT = Projectile velocity in the Z direction

PTDOT = Projectile velocity in the θ direction (radians/time)

TRDOT = Target velocity in the R direction

TZDOT = Target velocity in the Z direction

TTDOT = Target velocity in the θ direction

RDET = Radial coordinate of the detonation (distance)

ZDET = Axial coordinate of the detonation

Integration Time Increment Card (6F10.0)

DT1 = Integration time increment (Δt in equations of motion in subsection 2.5) for the first cycle. This must be less than the time required to travel across the minimum altitude of each triangular element at the sound speed of the material in that element.

DTMAX = The maximum integration time increment which will be used for the equations of motion. If Δt from Equation (42) is greater than DTMAX, it will be redefined at Δt = DTMAX.

DTMIN = The minimum integration time increment allowed. If Δt from Equation (42) is less than DTMIN, the results will be written onto the restart tape and the run will stop.

SSF = The fraction of the sound speed transit time used for the integration time increment. This is identical to C_t in Equation (42) and must be less than unity.

TMAX   = The maximum time the problem is allowed to run. This time
           refers to the dynamic response of the system, not the central
           processor time (CPMAX) defined in the Identification card.

TBURN   = The time at which the detonation begins at RDET, ZDET.

Data Output Cards (4F10. 0, 3I5)

These cards are used to specify various forms of output data at selected
times. The last card must be for a time greater than TMAX, even though
output will not be provided for that specific time.

TIME   = Time at which output data will be provided.

ECHECK = A code which governs the printed output. The three following
           options are provided:

    1)   If ECHECK is greater than 1000. , the individual
         node data and element data will not be printed.
         Only system data such as cg positions, momenta,
         kinetic energies and average velocities are pro-
         vided for the projectile, target and entire system.

    2)   If ECHECK is positive (includes 0.) and less than
         1000. , the system data and individual node data
         will be printed. Individual solid-liquid element
         data will be printed for all elements which have
         an equivalent plastic strain (Equation (13)) equal
         to or greater than ECHECK. For example, if
         ECHECK = 0. , all element data will be printed.
         If ECHECK = 0. 5, only those elements with
         equivalent plastic strains equal to or greater

than 0. 5 will have data printed.   If ECHECK = 999. ,
no element data will be printed.

3)   If ECHECK is negative, the system data and indiv-
     idual node data will be printed.   The individual
     element data will be printed only for those elements
     which are plastic or failed.   Data for the elastic
     elements will not be printed.

BCHECK = A code which governs the printed output for explosive elements.
Individual element data will be printed for all explosive ele-
ments which have a burn fraction (Equation (30)) equal to or
greater than BCHECK.   If BCHECK = 0. all explosive elements
data will be printed.   If BCHECK = 0. 5, only those explosive
elements with burn fractions equal to or greater than 0. 5 will
have data printed.

RDAMP = The radial damping constant, C_D, in Equation (38).   This damp-
ing term acts until the time specified in the following Data Out-
put card.

ILOAD = 1 will compute internal loads in a cylindrical projectile.   This
option can only be used if NTOP, NBOT and NRING are properly
defined in the Miscellaneous card.   Will not compute if left
blank.

ISAVE = 1 will write results on Tape 2 for possible restart runs or state
plots.   Will not write results if left blank.

IDATA = 1 will write system data on Tape 3 for possible time plots.
Will not write system data if left blank.

With the exception of the special shapes, this completes the description of
the input data for an initial run.   Various types of special shapes can be
generated for either the projectile or the target.   The node and element

53

data for these special shapes are entered individually in the locations identified in Figure 11. A description of the special shapes data follows.

Identification Card for Rod Nodes (4I5, 3F10.0)

The rod geometry descriptions are given in Figure 13. The axi-symmetric rod geometry is generated about the Z axis as shown. If the inner radius coincides with the Z axis (R = 0), a solid rod is generated and the radius is restrained in the R direction. If the inner radius does not coincide with the Z axis, a hollow rod is generated and there are no restraints.

1 = Identification number for rod geometry.

N1 = The node number of the inner radius node at the top surface of the rod. The nodes of the rod are numbered consecutively beginning with N1. They are numbered in horizontal rows (increasing in the radial direction) beginning at the top and working downward.

NRING = The number of vertical rings of nodes. The maximum allowable number of rings is 16.

NPLN = The number of horizontal rows of nodes.

ZTOP = The Z coordinate at the top of the rod.

ZBOT = The Z coordinate at the bottom of the rod.

EXPAND = Factor by which the vertical distance between adjacent nodes changes. Factor applies from top to bottom. Same as described for the Projectile Node Data cards.

Figure 13.   Rod Shape Geometry

Top Radii Cards for Rod Nodes (8F10. 0)

RT (1) - RT (NRING) = Radii of the rings at the top of the rod.

Bottom Radii Cards for Rod Nodes (8F10. 0)

RB (1) - RB (NRING) = Radii of the rings at the bottom of the rod.

Identification Card for Nose Nodes (3I5, 5X, F10. 0)

The nose geometry descriptions are given in Figure 14. The axi-symmetric geometries for rounded and conical nose shapes are also generated about the Z axis (pointed downward) and the centerline nodes are restrained in the radial direction. The nodes at the rod-nose interface are not generated with the nose generator and must therefore be generated with the rod generator.

INOSE = $\begin{cases} 2 \text{ Identifies a rounded nose shape.} \\ 3 \text{ Identifies a conical nose shape.} \end{cases}$

N1   = The node number of the centerline node at the top of the nose at the rod interface. This is identical to the bottom center-line node of the rod. The nodes are numbered consecutively in a clockwise direction (excluding the interface nodes) begin-ning with the entire center ring and expanding outward.

NRING = Number of rings of nodes in the nose shape. Note that the number of rings of nodes in the nose is one less than the num-ber of rings of nodes in the matching rod at the interface. The maximum allowable number of rings is 15.

ZTOP   = The Z coordinate at the top of the nose. This is identical to ZBOT for the rod shape at the rod interface.

56

ROUNDED NOSE (ISHAPE = 2)

ROD

NODE [N1]

NODE [N1 + NRING + 1]

RT(1) RT(2)   RT(NRING) ← RADII AT INTERFACE

1   2   NRING ← RINGS OF NODES

ZTOP — ← ROD-NOSE INTERFACE

ZM(1) —

ZM(2) —

NODE [N1 + NRING]

ZM(NRING) — NODE [N1 + NRING + NTOT]

CONICAL NOSE (ISHAPE = 3)

ROD

ELEMENT [ELE1]   1   2   NRING

1 {

2 {

RINGS (LAYERS) OF ELEMENTS

NRING {   ELEMENT [ELE1 + ETOT - 1]

NUMBER OF RINGS (NRING)	NUMBER OF NODES (NTOT)*	NUMBER OF ELEMENTS (ETOT)
1	2	2
2	6	8
3	12	18
4	20	32
5	30	50
6	42	72
7	56	98
8	72	128
9	90	162
10	110	200
11	132	242
12	156	288
13	182	338
14	210	392
15	240	450

* DOES NOT INCLUDE INTERFACE NODES

NODES AND ELEMENTS ARE NUMBERED CONSECUTIVELY, IN A CLOCKWISE DIRECTION, BEGINNING WITH THE ENTIRE CENTER RING AND EXPANDING OUTWARD. THIS DOES NOT APPLY TO THE INTERFACE NODES SINCE THEY ARE NOT GENERATED FOR THE NOSE SHAPES, BUT ARE USED ONLY FOR REFERENCE.
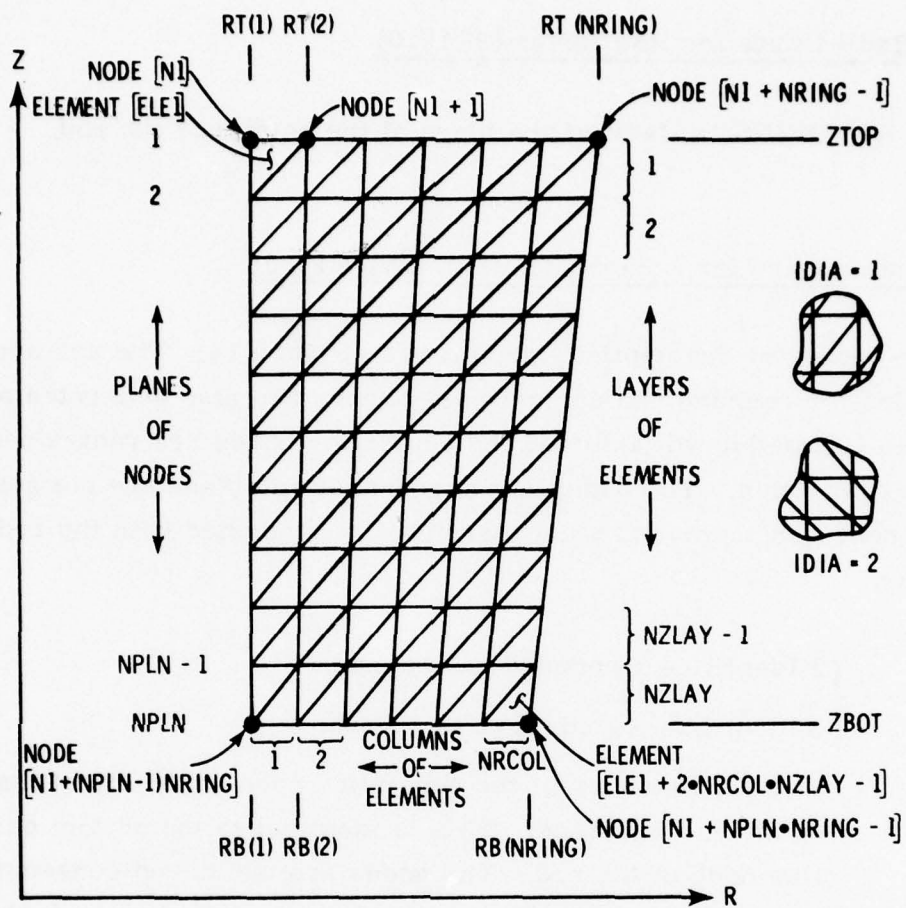
Figure 14. Nose Shape Geometry

57

Top Radii Cards for Nose Nodes (8F10.0)

RT (1) - RT (NRING) = Radii of the rings at the top of the nose. Only solid (not hollow) nose shapes are allowed. Note that the centerline node is always on the Z axis and that RT (1) is the adjacent node.

Minimum Z Coordinate Cards for Nose Nodes (8F10.0)

ZM (1) - ZM (NRING) = Minimum Z coordinates (at R = 0) for the rings in the nose shape.

Card for Sphere Nodes (3I5, 5X, 2F10.0)

The sphere geometry descriptions are given in Figure 15. The axi-symmetric sphere geometry is generated about the Z axis and the centerline nodes are restrained in the radial direction.

4   =   Identification number for sphere geometry.

N1   =   The node number at the center of the sphere. The nodes are numbered consecutively, in a clockwise direction, beginning with the inner ring and expanding outward with equal radial spacing.

NRING   =   Number of rings of nodes. The maximum allowable number of rings is 15.

ZTOP   =   The Z coordinate at the top of the sphere.

ZBOT   =   The Z coordinate at the bottom of the sphere.

58

NUMBER OF RINGS (NRING)	NUMBER OF NODES (NTOT)	NUMBER OF ELEMENTS (ETOT)
1	6	4
2	15	16
3	28	36
4	45	64
5	66	100
6	91	144
7	120	196
8	153	256
9	190	324
10	231	400
11	276	484
12	325	576
13	378	676
14	435	784
15	496	900

NODES AND ELEMENTS ARE NUMBERED CONSECUTIVELY, IN A CLOCKWISE DIRECTION, BEGINNING WITH THE CENTER RING AND EXPANDING OUTWARD
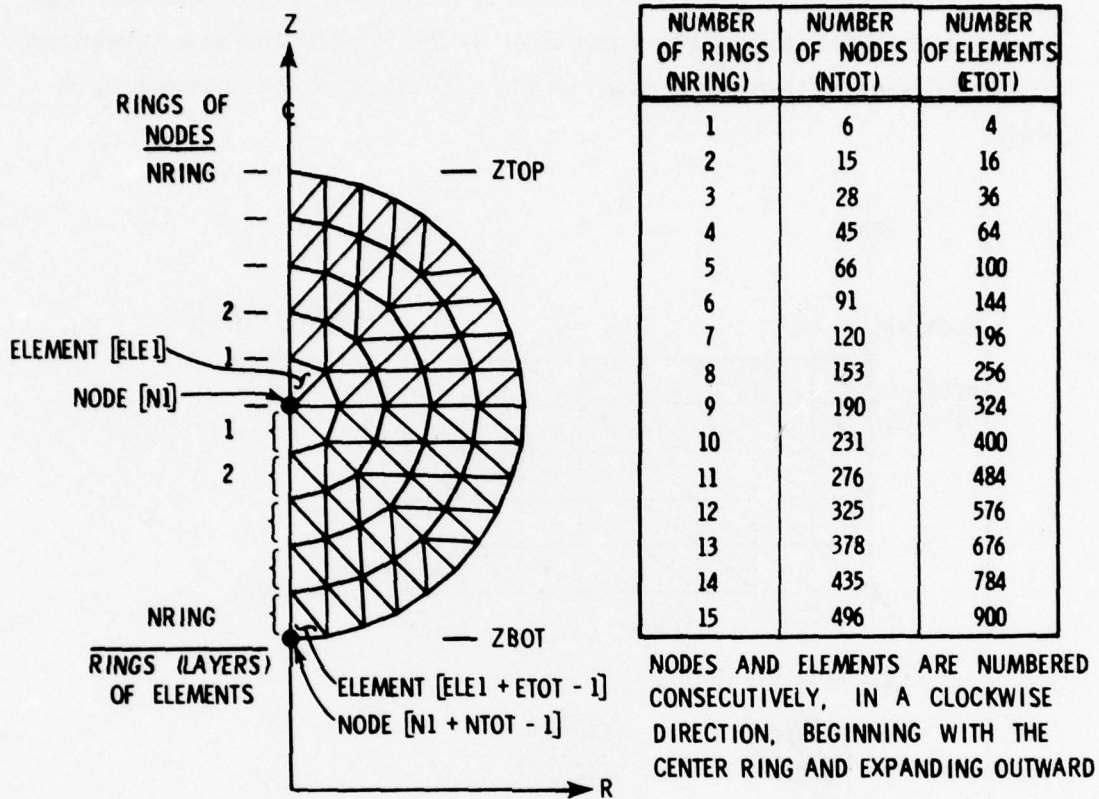
Figure 15.   Sphere Geometry

Identification Card for Flat-Plate Nodes (2I5)

The flat-plate geometry descriptions are given in Figure 16.   The flat-plate geometry is generated for a rectangular cross section as shown.

5   = Identification number for flat-plate geometry.

N1 = The node number of the first node at R = RMIN and Z = ZMAX. The nodes are generated in rows parallel to the R axis and are numbered consecutively within each row, in the direction of the increasing R axis.
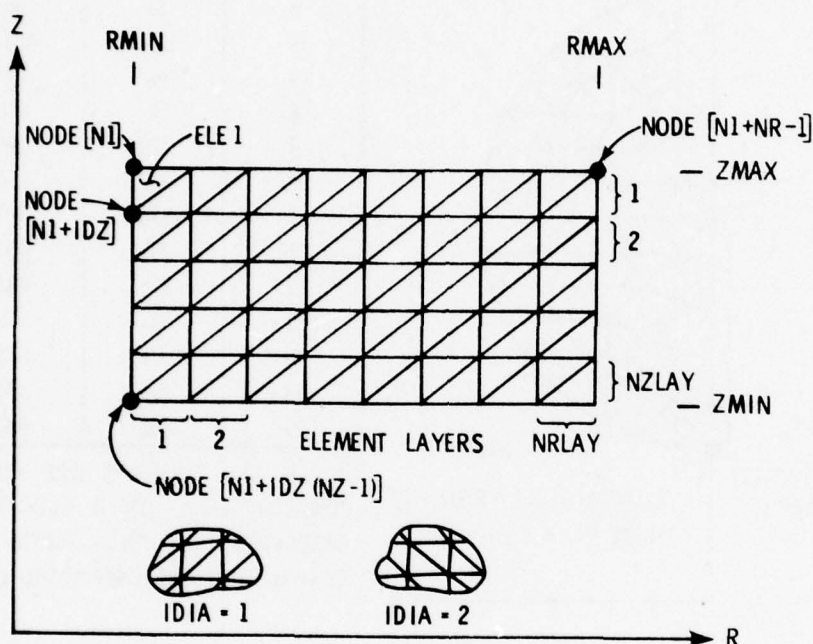
Figure 16. Flat-Plate Geometry

Description Card for Flat-Plate Nodes (4I5, 6F10.0)

NR   = The number of nodes in the R direction.

NZ   = The number of nodes in the Z direction.

IDZ = The node number increment between adjacent nodes when moving downward parallel to the Z axis. If the entire plate is formed with one node shape, the IDZ should be equal to NR. For multiple-plate shapes it should be equal to the total number of nodes in the R direction.

IRFIX = 1 will radially restrain all nodes on the Z axis (R = 0).

RMAX = The maximum coordinate in the R direction.

RMIN = The minimum coordinate in the R direction.

ZMAX = The maximum coordinate in the Z direction.

ZMIN = The minimum coordinate in the Z direction.

R-EXPAND = Factor by which the distance between adjacent nodes changes in the increasing R direction from RMIN to RMAX.

Z-EXPAND = Factor by which the distance between adjacent nodes changes in the decreasing Z direction from ZMAX to ZMIN.

Identification Card for Rod Elements (6I5)

1 = Identification number for rod geometry.

N1 = The node number of the inner radius node at the top surface of the rod.

NRCOL = The number of vertical columns of elements. Note that NRCOL = NRING - 1 for rod geometry. The maximum allowable number of columns of elements is 15.

NZLAY = The number of horizontal layers of elements. Note that NZLAY = NPLN - 1.

IDIA = Code for orientation of diagonals as shown.

61

ELE1 = The element number of the first element (contains node N1).
The elements are numbered consecutively and are generated
in vertical columns beginning with the top layer 1 and ending
at bottom layer NZLAY. The entire inner radial column is
generated before the adjacent outer radius column is gener-
ated etc.

Material Card for Rod Elements (15I5)

M (1) - M (NRCOL) = Material numbers for the columns of elements.

Identification Card for Nose Elements (3I5, 10X, I5)

The nose geometry descriptions are given in Figure 14.

INOSE = $\begin{cases} 2 \text{ identifies a rounded nose shape.} \\ 3 \text{ identifies a conical nose shape.} \end{cases}$

N1 = The node number at the centerline node at the top of the
nose at the rod interface. This is identical to the bottom
centerline node of the rod.

NRING = Number of rings of elements (and nodes) in the nose shape.
The maximum allowable number of rings is 15.

ELE1 = The element number of the first element in the nose shape.
The elements are numbered consecutively, in a clockwise
direction, beginning with the entire center ring and expand-
ing outward.

Material Card for Nose Elements (15I5)

M (1) - M (NRING) = Material numbers for the rings of elements.

Card for Sphere Elements (3I5, 10X, 2I5)

The sphere geometry descriptions are given in Figure 15.

4   =   Identification number for sphere geometry.

N1   =   The node number at the center of the sphere.

NRING   =   Number of rings of elements. The maximum allowable number of rings is 15.

ELE1   =   The element number of the first element in the sphere. The elements are numbered consecutively, in a clockwise direction, beginning with the inner ring and expanding outward.

MATL   =   The material number for all elements in the sphere.

Card for Flat-Plate Elements (7I5)

The flat-plate descriptions are given in Figure 16.

5   =   Identification number for flat-plate geometry.

N1   =   The node number of the first node at R = RMIN and Z = ZMAX

NRLAY   =   Number of vertical layers (columns) of elements.

NZLAY   =   Number of horizontal layers of elements.

IDIA   = Code for orientation of diagonals as shown.

ELE1   = The element number of the first element in the plate (contains
               node N1). The elements are numbered consecutively in hori-
               zontal rows expanding outward. After a row is complete, the
               next lower row is numbered in a similar manner.

MATL   = The material number for all elements in the plate.

4.2 INPUT DATA FOR A RESTART RUN

A restart run is one which reads data from Tape 2. These data must have
been previously generated by setting ISAVE = 1 on a Data Output card for an
initial geometry run or a previous restart run. The descriptions which
follow are for the input data in Figure 11.

Identification Card (3I5, 5X, F10.0)

CASE   = Case number for run identification. This does not have to
               be identical to that of the previous run.

CYCLE   = The cycle number at which the restart occurs. The cycle
               numbers for which restart files are written are given in the
               printed output of the previous run.

IWIND =   { 0 will not rewind Tape 2 after the program has read the
               restart data. This allows the entire run (from time = 0)
               to be saved on one tape.

               1 will rewind Tape 2 after the program has read the restart
               data. Previously generated data for lower cycle numbers
               will then be erased.

64

CPMAX   = Central processor time (hours) at which the results will be
            written onto a restart tape and the run will stop. This fea-
            ture will be by-passed if CPMAX = 0.

Integration Time Increment Card (3F10. 0)

DTMIN   = The minimum integration time increment which is allowed.
            If Δt from Equation (42) is less than DTMIN, the results will
            be written onto the restart tape and the run will stop.

SSF   = The fraction of the sound speed transit time used for the in-
            tegration time increment. This is identical to C_t in Equation
            (42) and must be less than unity.

TMAX   = The maximum time the problem is allowed to run. This time
            refers to the dynamic response of the system, not the central
            processor time (CPMAX) defined in the Identification Card.

Data Output Cards (4F10. 0, 3I5)

Identical to the Data Output cards for the initial run input data described in
subsection 4. 1.

4.3 INPUT DATA FOR STATE PLOTS

Input data for state plots are shown in Figure 11. This plotting program
reads data from Tape 2 which must be previously generated by setting
ISAVE = 1 on a Data Output Card for an initial geometry run or a restart
run. Five types of plots are available; each plot requires a State Plot

Identification card and another card to input the data for the specific type of plot requested. The data must be input in groups of two cards and the requested cycle numbers must be equal to or greater than the previously requested cycle number. Program ends with a blank card.

State Plot Identification Card (2I5, 4F10. 0)

This identifies the type of plot and the coordinates.

TYPE   =   A code to specify the type of plot requested.

             TYPE = 1 gives a geometry plot

             TYPE = 2 gives a stress field plot

             TYPE = 3 gives a pressure field plot

             TYPE = 4 gives a strain field plot

             TYPE = 5 gives a velocity field plot

CYCLE =   The cycle number of the plot which is desired. The cycle numbers of the data written on Tape 2 are given in the printed output of the main program.

ZMAX =   The maximum axial Z coordinate on the plot. The Z coordinate (ZMAX to ZMIN) is 10.0 inches long and is divided into 10 equal increments.

ZMIN   =   The minimum Z coordinate on the plot.

RMAX =   The maximum radial R coordinate on the plot. The R coordinate (RMAX to RMIN) can be any length and the scale is equal to that of the Z coordinate.

RMIN   =   The minimum R coordinate on the plot.

Deformed Geometry Plot Card (3A6, 2X, 4I5)

This gives plots of geometry composed of triangular elements.

TITLE = The title which is written on the plot. The time and cycle number are also written on the plot.

EDGE = A code to specify if an outline of the geometry should be plotted.

   EDGE = 0 gives no outline.

   EDGE = 1 gives an outline of the actual geometry.

   EDGE = -1 gives an outline of the mirror image of the actual geometry for axi-symmetric cases.

   EDGE = 2 gives an outline of both the actual geometry and the mirror image of the actual geometry.

IE = 1 will write "E" at the center of all elements which are in the elastic range. Will not write if it is left blank.

ID = 1 will write "P" at the center of all elements which are in the plastic flow range. Will not write if it is left blank.

IF = 1 will write "F" at the center of all elements which are failed (no shear or tensile stress). Will not write if it is left blank.

Stress Field Plot Card (3A6, 2X, 2I5, 5F10. 0)

This gives plots of lines of constant equivalent stress given by Equation (23).

TITLE = The title which is written on the plot.

EDGE = A code to specify if the outline of the geometry should be plotted. See description given for the Deformed Geometry Plot card.

NLINE = The number of lines of constant stress to be plotted. Must be
          1, 2, 3, 4 or 5.

STRESS (1) - STRESS (5) are the specific values of lines of constant stress.

Pressure Field Plot Card (3A6, 2X, 2I5, 5F10. 0)

Same as the Stress Field Plot card except the net pressure (hydrostatic plus
artificial viscosity) is plotted.

Strain Field Plot Card (3A6, 2X, 2I5, 5F10. 0)

Same as the Stress Field Plot card except the equivalent plastic strain
(Equation (13)) is plotted.

Velocity Field Plot Card (3A6, 2X, I5, 5X, F10. 0)

This plots velocity vectors based on the position, velocity and direction of
the velocity of the nodes.

TITLE   = The title which is written on the plot.

EDGE   = A code to specify if the outline of the geometry should be
           plotted. See description given for the Deformed Geometry
           Plot card.

VSCALE = The velocity which will give a velocity vector which has a
           length of 1. 0 inch.

68

4.4 INPUT DATA FOR TIME PLOTS

Input data for time plots are shown in Figure 11. This plotting program
reads data from Tape 3 which must be previously generated by setting
IDATA = 1 on the Data Output cards for an initial run or a restart run.
The variables plotted are shown in Figure 11. They are plotted as a
function of time at the various times specified on the Data Output cards.
Any or all of the 11 varables can be plotted. Each plot contains data for
the projectile, the target, and the total system (projectile plus target).
End with a blank card.

TYPE   =   A code to specify the variable to be plotted. Code is given in
                Figure 11.

TMAX =   The maximum time included in the plot (micro-seconds).

TMIN   =   The minimum time included in the plot (micro-seconds).

VMAX =   The maximum value of the specified variable to be plotted.

VMIN   =   The minimum value of the specified variable to be plotted.

TITLE =   The title which is printed on the plot.

4.5 OUTPUT DATA DESCRIPTION

The output data are generally described using the terminology of
this report. A summary of the printed output for an initial run is as
follows:

- All input data are printed exactly as read.

- Material data are printed for the input data.

- All the geometric input data are printed in a form similar to that used to read the data.

- For each node, the initial coordinates, mass and restraints are printed. The slave nodes are identified by adding a "1" before the RZT restraint. (Example: If the RZT restraint is 100, the nodes are restrained in the radial direction. If the RZT restraint is 1100, it is a slave node with the same restraint.)

- For each element, the three nodes, cross-sectional area, volume and material number are printed.

- A summary of the initial geometry and impact/detonation conditions is printed. Included are the number of nodes and elements, mass, cg positions, velocities, detonation location, energies and integration time increment data.

- For each integration time increment selected data are printed. These consist of cycle number (CYCLE), the time (TIME), the integration time increment (DT), the element number which governs the time increment (ECRIT), the total system kinetic energy (TOTAL K.E.), the projectile kinetic energy (PROJ K.E.), the total axial Z momentum of the system (TOTAL MVZ), the projectile axial Z momentum (PROJ MVZ), the total spin momentum of the system (TOTAL MVS), the projectile spin momentum (PROJ MVS), and the total energy in the system (TOT ENERGY). If ECRIT = 0, the integration time increment calculated by Equation (42) is either greater than DTMAX, or greater than 1.1 times the integration time increment for the previous cycle. If the problem is plane strain (instead of axi-symmetric), momenta in the R direction are given in place of spin momenta (TOTAL MVS, PROJ MVS).

70

- Node data are printed at the selected times specified on the Data Output Cards. These data include the node number (NODE), the coordinates (R, Z, T), the velocities (RDOT, ZDOT, TDOT), and the accelerations (RDD, ZDD, TDD). If the acceleration data are not printed, this indicates the node is a slave node which is currently in contact with the master surface.

- Element data are also printed at the selected times on the Data Output cards. These data consist of the element number (ELE), the relative volume (RELVOL), the volumetric strain (DVOL), the volumetric strain rate (DVDOT), the equivalent plastic strain (EPBAR) given in Equation (13), the equivalent stress (SEFF) given in Equation (23), the normal deviator stresses (SR, SZ, ST) given in Equations (17) - (19), the shear stresses (SRZ, SRT, SZT) given by Equations (20) - (22), the pressure (PRESURE) given by Equation (26) or (29), the artificial viscosity [Q (VIS)] given by Equation (31), the temperature (TEMP) given by Equation (25) and the burn fraction (BURNFR) given by Equation (30).

- Internal loads can be obtained for axi-symmetric rod projectiles at selected times if the nodal geometry is consistent with the geometry generator for rods and if ILOAD = 1 on the Data Output cards. The output is given along the centerline of the projectile from nodes NTOP to NBOT as specified on the Miscellaneous card. Included are the node numbers (NODE), the axial coordinate of the node (Z), the compressive axial load (AXIAL LOAD) and the torque (TORQUE). The results are valid only along the free portion of the projectile and are not valid for the portions which are in contact with the target.

71

- A summary of system data is printed for selected time specified on the Data Output cards. Data are given for the projectile, target and total system. These data consist of mass, cg, kinetic energy, internal energy, total energy (kinetic plus internal), plastic work, momenta in Z direction, net velocity in Z direction, angular momenta about Z axis (linear momenta in R direction if plane strain), angular velocity about Z axis (linear velocity in R direction if plane strain), maximum Z coordinate and minimum Z coordinate.

4.6 DIAGNOSTICS

The following diagnostics are given prior to discontinuing the run.

- ILLEGAL RESTRAINT ON SLAVE NODE -- This means a slave node has restraints in the Z or θ directions or it is restrained in the R direction, but the radial coordinate is not equal to the radial coordinate of the first or last master node.

  This also occurs if node is designated as a slave node more than one time.

- ILLEGAL SLAVE ELEMENT -- A slave element does not have exactly two slave nodes.

- ILLEGAL REQUEST FOR NODE SHAPE -- A request is made for a special node shape which does not have an identification number of 1, 2, 3, 4 or 5.

- ILLEGAL REQUEST FOR ELEMENT SHAPE -- A request is made for a special element shape which does not have an identification number of 1, 2, 3, 4 or 5.

- MINIMUM TIME INCREMENT HAS BEEN VIOLATED -- This means the time increment given by Equation (43) is less than specified by DTMIN on the Integration Time Increment

72

card. The results are written on Tape 2 and/or Tape 3 if previously specified (they are not printed). If it is desired to continue the run to later times, DTMIN must be decreased for the next restart run.

- CP TIME LIMIT EXCEEDED -- This means the central processor time is greater than specified by CPMAX on the Identification card. The results are then printed and written on Tape 2 and/or Tape 3 if previously specified.

- ENERGY CHECK INDICATES NUMERICAL INSTABILITY -- This means the kinetic energy of the system is at least 10 percent greater than the initial energy (kinetic plus internal explosive energy) of the system. Since this is not physically possible, the run must be numerically unstable. The results are printed and written on Tape 2 and/or Tape 3 if previously specified.

- REQUESTED CYCLE NOT FOUND ON TAPE -- This means a restart tape (Tape 2) does not have data for cycle number specified on the Identification card.

4.7 CENTRAL PROCESSOR TIME ESTIMATES

For various problems run on a Honeywell 6080 computer, the EPIC-2 program has used approximately 0.0045 central processor second per node per cycle.

4.8 CENTRAL MEMORY STORAGE REQUIREMENTS AND ALTERATIONS

The EPIC-2 program is currently limited to 10 materials (five solid-liquid and five explosive), 1000 nodes, 2000 elements and five sliding surfaces, each with a maximum of 100 master nodes, 100 slave nodes and 100 slave elements. This requires 76K Central Memory Storage on a Honeywell 6080 computer. These limits can be altered by altering the appropriate common arrays in all subroutines which contain those arrays.

REFERENCES

1. Wilkins, M. L. , "Calculation of Elastic-Plastic Flow," Methods in Computational Physics, Vol. 3, edited by B. Alder, S. Fernback and M. Rottenberg, Academic Press, New York, N.Y. , 1964.

2. Von Neumann, J. and Richtmyer, R. D. , "A Method for the Numerical Calculation of Hydrodynamic Shocks," Journal of Applied Physics, Vol. 21, 1950.

3. Walsh, R. T. , "Finite Difference Methods," Dynamic Response of Materials to Intense Impulsive Loading, edited by P. C. Chou and A. K. Hopkins, Air Force Materials Laboratory, 1972.

4. Bertholf, L. D. , and Benzley, S. E. , "TOODY II, A Computer Program for Two-Dimensional Wave Propagation," SC-RR-68-41, Sandia Laboratories, Albuquerque, New Mexico, 1968.

5. Wang, C. T. , Applied Elasticity, McGraw-Hill, New York, 1953.

6. Johnson, G. R. , "Analysis of Elastic-Plastic Impact Involving Severe Distortions," Journal of Applied Mechanics, ASME, Vol. 98, Series E, Sept. 1976.

7. Johnson, G. R. , "Liquid-Solid Impact Calculations with Triangular Elements," Journal of Fluids Engineering, ASME, Vol. 99, Series I, Sept. 1977.

APPENDIX A
SAMPLE PROBLEM

Input data for a sample problem is provided in Figure A-1, and a geometry plot is shown in Figure A-2. This problem consists of a copper rod with a hemispherical nose impacting a steel plate at 60,000 inch/sec. The total length of the rod is 4.9 inches and the radius is 0.5 inch; the thickness of the plate is 0.5 inch and the radius is 4.0 inches. The nodes in the rod are generated in two sections to allow expanded spacing near the aft end of the rod; likewise, the nodes in the plate are generated in two sections. The nodes in the forward end of the rod are designated as slave nodes, and the nodes on the top surface of the plate are designated as master nodes. This problem contains 372 nodes and 600 elements.

```
100      1      1      1         .1                      .000734
         .000831                                 4100 0.
         360000.                                 93000 0.
         6350000.                                     0.
              0.                                 1600 0.
         20300.                                  2030 0.
         65300.                                        .3
              .3                                 677 0.
         21800.                                       0.
              0.                                      0.
              0.                                      1.
              1.                                      0.
              0.                              242000 00.
         20235000.                            59578000.
         32507000.                            740810 00.
         64254000.                                1 67
              2.00                                   .2
               .2                                   4.0
              4.0                                    .7
              999.                               999.
              999.                               999.
              2.                                  70.
              70.
1        1      0      1    101   299    6
         1.            1.

1   101      6     13         4.9       2.4         .9
    0.             .1          .2        .3         .4         .5
    0.             .1          .2        .3         .4         .5
1   177      6     21         2.3       .5         1.0
    0.             .1          .2        .3         .4         .5
    0.             .1          .2        .3         .4         .5
2   299      5                .5
     .1             .2          .3        .4         .5
     .4             .3          .2        .1         0.

     1.             1.

5   601
15    6     23      1         1.4       0.        0.        -.5       1.0       1.0
5   615
8     6     23      0         4.        1.5       0.        -.5       1.4       1.0


1   101      5     33      2    101
1     1      1      1      1
2   299      5                501
1     1      1      1      1

5   601     22      5      2    601     3

2
601   602     0
12     46     0
601   602   603   604   605   606   607   608   609   610   611   612
287   288   289   290   291   292   293   294   295   296   297   298   299   300   301   302
303   304   305   306   307   308   309   310   311   312   313   314   315   316   317   318
319   320   321   322   323   324   325   326   327   328   329   330   331   332   333   334
    0.    -60000.        0.        0.        0.        0.
.0000001   .0000005   .00000001       .5   0000002
    0.      1111.        0.        0.    1     1     0
    1.
```
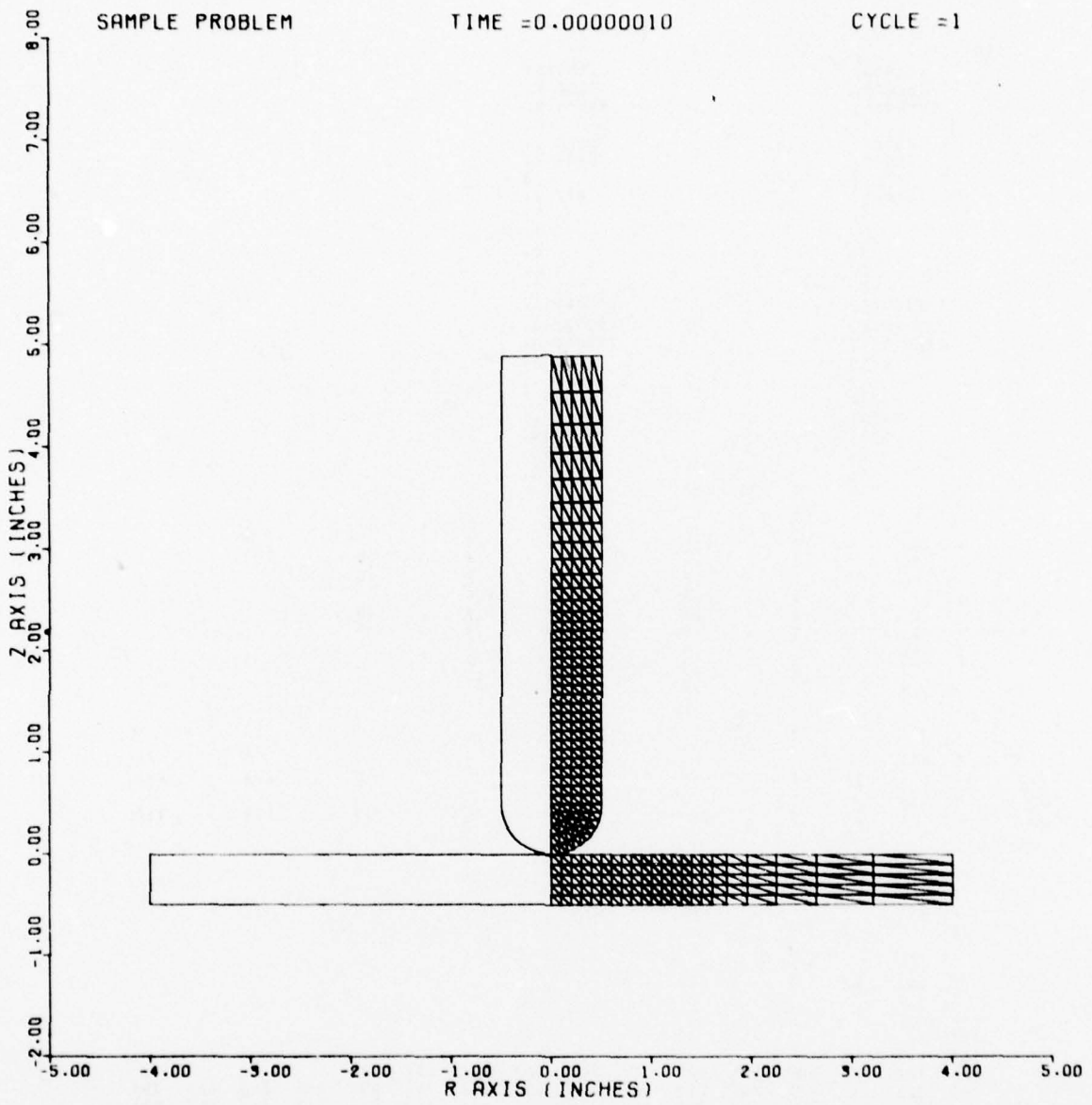
Figure A-1. Input Data for the Sample Problem

77

Figure A-2. Initial Geometry Plot of the Sample Problem

78

DISTRIBUTION LIST

No. of Copies	Organization	No. of Copies	Organization
12	Commander Defense Documentation Center ATTN: DDC-TCA Cameron Station Alexandria, VA 22314	1	Commander US Army Communications Research and Development Command ATTN: DRDCO-SGS Fort Monmouth, NJ 07703
1	Director Defense Advanced Research Projects Agency ATTN: Tech Info 1400 Wilson Boulevard Arlington, VA 22209	2	Commander US Army Missile Research and Development Command ATTN: DRDMI-R DRDMI-RBL Redstone Arsenal, AL 35809
1	Director Defense Nuclear Agency ATTN: MAJ Spangler Arlington, VA 22209	1	Commander US Army Missile Materiel Readiness Command ATTN: DRSMI-AOM Redstone Arsenal, AL 35809
1	Commander US Army Materiel Development and Readiness Command ATTN: DRCDMD-ST, N. Klein 5001 Eisenhower Avenue Alexandria, VA 22333	1	Commander US Army Tank Automotive Research & Development Cmd ATTN: DRDTA-UL Warren, MI 48090
1	Commander US Army Aviation Research and Development Command ATTN: DRSAV-E 12th and Spruce Streets St. Louis, MO 63166	1	Commander US Army Armament Materiel Readiness Command ATTN: DRSAR-LEP-L, Tech Lib Rock Island, IL 61299
1	Director US Army Air Mobility Research and Development Laboratory Ames Research Center Moffett Field, CA 94035	2	Commander US Army Armament Research and Development Command ATTN: DRDAR-TSS (2 cys) Dover, NJ 07801
1	Commander US Army Electronics Research and Development Command Technical Support Activity ATTN: DELSD-L Fort Monmouth, NJ 07703	4	Commander US Army Armament Research and Development Command ATTN: Mr. V. Guadagno Mr. R. Davitt Dr. J. T. Frasier Mr. G. Demitrak Dover, NJ 07801

DISTRIBUTION LIST

DISTRIBUTION LIST

No. of Copies	Organization
4	Commander Naval Research Laboratory ATTN: Mr. W. J. Ferguson Dr. C. Sanday Dr. H. Pusey Dr. F. Rosenthal Washington, DC 20375
1	Superintendent Naval Postgraduate School ATTN: Dir of Lib Monterey, CA 93940
1	AFOSR (W. J. Walker) Bolling AFB, DC 20332
2	ADTC/DLJW (MAJ D. Matuska; LTC J. Osborn) Eglin AFB, FL 32542
1	AFFDL (FDT) Wright-Patterson AFB, OH 45433
1	AFML (Dr. T. Nicholas) Wright-Patterson AFB, OH 45433
3	ASD (YH/EX; John Rievley; XROT, Gerald Bennett; ENFTV, Matt Kolleck) Wright-Patterson AFB, OH 45433
1	Headquarters National Aeronautics and Space Administration Washington, DC 20546
4	Director National Aeronautics and Space Administration Langley Research Center Langley Station Hampton, VA 23365

No. of Copies	Organization
1	Director National Aeronautics and Space Administration Manned Spacecraft Center ATTN: Lib Houston, TX 77058
1	Director Jet Propulsion Laboratory ATTN: Lib (TD) 4800 Oak Grove Drive Pasadena, CA 91103
3	Director Lawrence Livermore Laboratory ATTN: Dr. R.H. Toland, L-424 Dr. M. L. Wilkins Dr. R. Werne Livermore, CA 94550
1	Aeronautical Research Assoc. of Princeton, Inc. 50 Washington Road Princeton, NJ 08540
2	Aerospace Corporation ATTN: Mr. L. Rubin Mr. L. G. King 2350 E. El Segundo Blvd. El Segundo, CA 90009
1	Boeing Aerospace Company ATTN: Mr. R. G. Blaisdell (M.S. 40-25) Seattle, WA 98124
1	Dupont Experimental Labs ATTN: Mr. J. Lupton Wilmington, DE 19801
1	Effects Technology, Inc. 5383 Hollister Avenue P. O. Box 30400 Santa Barbara, CA 93105

DISTRIBUTION LIST

No. of Copies	Organization	No. of Copies	Organization

1   Falcon R&D
    ATTN: Mr. R. Miller
    1225 S. Huron Street
    Denver, CO 80223

2   Falcon R&D
    Thor Facility
    ATTN: Mr. D. Malick
          Mr. J. Wilson
    696 Fairmount Avenue
    Baltimore, MD 21204

1   FMC Corporation
    Ordnance Engineering Div
    San Jose, CA 95114

1   General Electric Company
    Armament Systems Dept.
    Burlington, VT 05401

1   President
    General Research Corporation
    ATTN: Lib
    McLean, VA 22101

1   Goodier Aerospace Corp.
    1210 Massillon Road
    Akron, OH 44315

1   H. P. White Laboratory
    Bel Air, MD 21014

3   Honeywell, Inc.
    Government and Aerospace
      Products Division
    ATTN: Mr. J. Blackburn
          Dr. G. Johnson
          Mr. R. Simpson
    600 Second Street, NE
    Hopkins, MN 55343

1   Kaman Sciences Corporation
    ATTN: Dr. P. Snow
    1500 Garden of the Gods Road
    Colorado Springs, CO 80933

1   Lockheed Corporation
    ATTN: Dr. C. E. Vivian
    Sunnyvale, CA 94087

1   Lockheed Huntsville
    ATTN: Dr. E.A. Picklesimer
    P. O. Box 1103
    Huntsville, AL 35809

1   Materials Research
      Laboratory, Inc.
    1 Science Road
    Glenwood, IL 60427

1   McDonnell Douglas Astronautics
    ATTN: Mail Station 21-2
          Dr. J. Wall
    5301 Bolsa Avenue
    Huntington Beach, CA 92647

1   Pacific Technical Corporation
    ATTN: Dr. F. K. Feldmann
    460 Ward Drive
    Santa Barbara, CA 93105

1   Philco-Ford Corporation
    Capistrano Test
    San Juan Capistrano, CA 92675

2   Physics International Company
    ATTN: Dr. D. Orphal
          Dr. E. T. Moore
    2700 Merced Street
    San Leandro, CA 94577

1   Rockwell International
    Autometics Missile Systems Div.
    ATTN: Dr. M. Chawla
    4300 E. 5th Avenue
    Columbus, OH 43216

DISTRIBUTION LIST

No. of Copies	Organization
3	Sandia Laboratories ATTN: Dr. W. Herrmann Dr. L. Bertholf Dr. J. W. Nunziato Albuquerque, NM 87115
1	Science Applications, Inc. 101 Continental Blvd, Suite 310 El Segundo, CA 90245
1	Science Applications, Inc. ATTN: G. Burghart 201 W. Dyer Rd (Unit B) Santa Ana, CA 92707
2	Systems, Science & Software ATTN: Dr. R. Sedgwick Ms. L. Hageman P. O. Box 1620 La Jolla, CA 92038
1	US Steel Corporation Research Center 125 Jamison Lane Monroeville, PA 15146
1	Drexel University Dept of Mechanical Engineering ATTN: Dr. P. C. Chou 32nd and Chestnut Streets Philadelphia, PA 19104
1	New Mexico Institute of Mining and Technology Terra Group Socorro, NM 87801
1	Forrestal Research Center Aeronautical Engineering Lab Princeton University ATTN: Dr. Eringen Princeton, NJ 08540

No. of Copies	Organization
3	Southwest Research Institute Dept of Mechanical Sciences ATTN: Dr. U. Lindholm Dr. W. Baker Dr. P. H. Francis 8500 Culebra Road San Antonio, TX 78228
3	Stanford Research Institute ATTN: Dr. L. Seaman Dr. D. Curran Dr. D. Shockey 333 Ravenswood Avenue Menlo Park, CA 94025
2	University of Arizona Civil Engineering Department ATTN: Dr. D. A. DaDeppo Dr. R. Richard Tucson, AZ 85721
4	University of California Los Alamos Scientific Lab ATTN: Dr. R. Karpp Dr. J. Dienes Dr. L. Germain Dr. B. Germain P. O. Box 808 Livermore, CA 94550
1	University of Dayton University of Dayton Research Institute ATTN: Mr. H. F. Swift Dayton, OH 45405
2	University of Delaware Department of Mechanical Engineering ATTN: Prof. J. Vinson Dean I. Greenfield Newark, DE 19711

DISTRIBUTION LIST

No. of Copies	Organization
1	University of Denver Denver Research Institute ATTN: Mr. R. F. Recht 2390 South University Boulevard Denver, CO 80210

Aberdeen Proving Ground

Dir, USAMSAA

Cdr, USATECOM
   ATTN: DRSTE-SG-H
          Mr. W. Pless
          Mr. S. Keithley